

# Synthesis and characterization of nanostructured calcium oxides supported onto biochar and their application as catalysts for biodiesel production

Jean-Pierre Dupont<sup>1</sup>, Maria González Fernández<sup>2</sup>, Eva Schmidt<sup>3</sup>

<sup>1</sup> Professor, Department of Sociology, Université Paris 1 Panthéon-Sorbonne, France

<sup>2</sup> Associate Professor, Department of Political Science, Universidad Complutense de Madrid, Spain

<sup>3</sup> Researcher, Institute for Social Research, Goethe University Frankfurt, Germany

## Abstract

Nanostructured calcium oxides supported onto biochar obtained by pyrolysis of avocado seeds were prepared, characterised and successfully used as catalysts to produce biodiesel from waste oils. The effect of increasing calcium load (5, 10 and 20 wt.%) was investigated. Elemental analysis, FTIR, XRD, SEM, BET, acid and basic sites were used to characterize the resulting carbon-based calcium oxides. Supported systems efficiently promoted the transesterification of oil with methanol, but differently from calcium oxide, they were easily recoverable and reusable for three cycles without any loss of activity. Kinetic data were better fitted by a pseudo-second order model with an activation energy of 39.9 kJ·mol<sup>-1</sup>. Thermodynamic parameters of activation energy were also determined for the transesterification reaction ( $\Delta^\ddagger G$ : 98.68-106.08 kJ·mol<sup>-1</sup>,  $\Delta^\ddagger H$ : 37.05 kJ·mol<sup>-1</sup> and  $\Delta^\ddagger S$ : -0.185 kJ·mol<sup>-1</sup>·K). Finally, reaction conditions were optimised using the desirability function applied on the response surface methodology analysis of a Box–Behnken factorial design of experiments. By carrying out the reaction at 99.5 °C for 5 h with 7.3 wt.% of catalyst and a molar ratio of methanol to oil

of 15.6, a FAME content over 96 % was achieved. Even starting from waste cooking oil, final biodiesel was conform to the main EN14214 specifications.

**Keywords:** Biodiesel; nanostructured catalysts; heterogeneous catalysis; waste cooking oil; FAME.

## 1. Introduction

With the growth of the global demand for energy and of environmental concerns due to the limited availability of the conventional fossil fuels, the use of alternative renewable energies has received significant attention in recent years [1,2]. Biodiesel is a “green fuel” which reveals very similar physical and chemical properties to petroleum derivatives [3–5]. In addition, it offers several advantages such as renewability, biodegradability, non-toxic emissions and the possibility to be directly used in unmodified diesel engines [6–8]. Biodiesel is a mixture of Fatty Acid Methyl Esters (FAME) typically produced by the transesterification of glycerides (vegetable oil and/or animal fats) with methanol, in presence of homogeneous alkaline catalysts such as sodium or potassium hydroxide, carbonates or alkoxides [9,10]. Furthermore, transesterification operated under alkaline homogeneous catalysis can be strictly applied on refined oils or highly pure fats: content of Free Fatty Acids (FFA) must not exceed 0.1-0.5 wt.% in order to avoid the formation of soaps [11,12]. On the other hand, homogeneous acid catalysts ( $\text{H}_2\text{SO}_4$ ,  $\text{HCl}$ ) are non-sensitive to the presence of FFA, and are therefore mostly applicable for low quality feedstocks such as waste cooking oils (WCO), raw animal fats and non-edible oils [13,14]. However, transesterification under acid catalysis is around 4000 times slower than the alkaline catalysis. For this reason, the use of mineral acids on an industrial scale is limited to pretreat acid oils in order to

convert FFA into FAME through a direct esterification, while the subsequent transesterification of glycerides is preferentially operated under homogeneous alkaline conditions. However, in this industrial process, alkaline catalysts are not reusable and a large amount of chemical waste is produced. Recently, the use of supercritical methanol was proposed for the direct esterification of FFAs [15,16]. The reaction was found to be complete in a very short time (5-15 minutes) and the purification is much simpler and environmentally friendly. However, the reaction requires high temperatures (270-350 °C) and pressures (10–25 MPa), thus resulting in high production costs. For this reason, most of industrial processes for the production of biodiesel from WCO are presently based on the two-step reaction scheme. To overcome the abovementioned limitations of the two-step approach, heterogeneous catalysts were studied and applied for biodiesel production [17,18]. These catalysts are not consumed during the reaction, so they can be easily recovered from end products and re-used for a number of cycles, introducing also significant benefits in the downstream, making the recovery of products simpler. Heterogeneous catalysts such as supported alkaline metal hydroxides [19,20], pure and mixed oxides [21,22], hydrotalcites [23,24], ion exchange resins [25,26], zeolites [27] and heteropolyacids [28] have been studied and proposed as substitutes for conventional homogeneous systems. Novel surface functionalized TiO<sub>2</sub> nano-catalysts [29], magnetically separable SO<sub>4</sub>/Fe-Al-TiO<sub>2</sub> solid acid catalyst [30], core-shell nanostructured heteropoly acid-functionalized metal-organic frameworks [31] and core-shell SO<sub>4</sub>/Mg-Al-Fe<sub>3</sub>O<sub>4</sub> magnetic catalysts [32] were shown to be suitable as catalysts in low grade oils to produce biodiesel. For instance, Gardy et al. [29] evaluated the effect of reaction parameters in the conversion of WCO using TiO<sub>2</sub>/Pr-SO<sub>3</sub>H. Under optimal conditions, a FAME yield of 98.3 % was obtained at 60 °C and 6 h of reaction with a molar ratio methanol to oil of 15 and catalyst concentration of 4.5 wt.%. SO<sub>4</sub>/Fe-Al-TiO<sub>2</sub> [30] achieved a FAME yield of 96 % at 90 °C after 2.5 h, using a molar ratio

methanol to oil of 10:1 and 3 wt.% of catalyst. In a study conducted by Jeon et al. [31], biodiesel production from rapeseed oil was evaluated by using heteropoly acids supported onto zeolitic imidazolate framework-8 (ZIF-8) nanoparticles. After 2 h of reaction at 200 °C, a conversion > 98 % into FAME was obtained with a molar ratio methanol to oil of 10 and 4 wt.% of catalyst.

However, the main challenge in this topic is the development of new effective and cheap heterogeneous catalysts. In this sense, calcium oxide (CaO) is the most widely investigated due to its high catalytic activity, strong basicity, relatively low solubility in methanol and its possible obtainment from natural and waste materials [33,34]. Several authors have reported the application of CaO as a catalyst for converting a number of vegetable oils, by obtaining a FAME yield > 90 % after the first cycle of reaction [35,36]. Liu et al. [37] studied the transesterification of soybean oil catalyzed by CaO as an heterogeneous catalyst and achieved a yield of 95 % at 65 °C using a molar ratio methanol to oil of 12:1, 8 wt.% of catalyst and reaction time of 3 h. Viola et al. [38] performed the same reaction on WCO at 65 °C and reached a conversion of 93 % after 80 minutes with a molar ratio methanol to oil of 6 and 5 wt.% of catalyst. In any case, there is a big question mark over the reuse of the catalyst for subsequent cycles. The leaching of CaO, inside the reaction medium, represents one of the most important reasons for its deactivation [39,40]. During the transesterification reaction, the catalyst can easily react with glycerol obtained as a co-product of the process, with the formation of calcium diglyceroxide. This compound is more soluble in methanol than CaO and hydrolyzes in the presence of moisture by producing the less active calcium hydroxide [41]. Furthermore, the presence of FFA in crude oils leads to the formation of calcium soaps, thus decreasing catalytic activity and resulting in further separation problems of final products [42]. Finally, the active sites of the catalyst can also be poisoned by the adsorption of water and carbon dioxide onto the surface, producing

hydroxides and carbonates [43]. To address these issues and to mitigate these possible complications, the research has been focused on the improvement of the catalytic performance of CaO, by mixing it with other metal oxides or anchoring CaO onto cheap inorganic [36] or organic supports [44,45]. Carbon-based materials are considered as ideal supports due to their low cost, high surface area and thermal stability [46–48]. They can be easily functionalized by the addition of acids and bases [49], or can be directly used as a support for alkaline earth metal oxides [50,51]. In addition, these materials are eco-friendly, biodegradable and can be directly produced from residual biomasses, thus further reducing the environmental impact of biodiesel production.

In recent years, the avocado production has grown rapidly in Mexico: 2.03 MMt were produced in 2017 [52] with this production that is expected to grow up to 2.14 MMt in 2030 [53]. The processing of avocado fruit involves considerable waste to be generated, the seeds in particular, which represent around 13-16 wt.% of the dry fruit [54]. For this reason, efforts are underway to develop integrated strategies for the exploitation of this resource. Biochar obtained from the pyrolysis of avocado seeds shows a relatively high porosity and an alveolar surface, whose pore size are capable of allocating and anchoring different metallic active species [55,56].

In this work, several nanostructured calcium oxide deposited onto biochar deriving from avocado seeds were synthesized, fully characterized and tested in the transesterification reaction of sunflower oil with methanol. The catalysts were synthesized by the precipitation method. The effect of calcium loaded onto the structure, morphology and the activity in biodiesel production were investigated. Once the most active catalyst had been identified, the best operative conditions were determined through a response surface methodology on a Box–Behnken factorial design of experiments. Molar ratio methanol to oil, catalyst concentration, temperature and reaction time were optimized with the aim of maximizing the production of FAME. Finally, these optimized

conditions were adopted for the transesterification of pretreated WCO (starting acidity =  $8.05 \pm 0.04$  mg KOH g<sup>-1</sup>), in which FFA were previously converted into methyl esters by direct esterification, using aluminum chloride hexahydrate ( $\text{AlCl}_3 \cdot 6\text{H}_2\text{O}$ ) as catalyst [57]. The final product was a biodiesel conform to EN14214 specifications, by confirming the validity of the entire process and allowing biodiesel production from low quality feedstocks to be achieved.

## 2. Materials and Methods

### 2.1 Reagents

All chemical reagents used in this work were of analytical grade and were used directly without further purifications or treatments. Calcium nitrate tetrahydrate ( $\text{Ca}(\text{NO}_3)_2 \cdot 4\text{H}_2\text{O}$ ,  $\geq 99\%$ ), aluminum chloride hexahydrate ( $\text{AlCl}_3 \cdot 6\text{H}_2\text{O}$ ,  $\geq 99\%$ ), sodium hydroxide (NaOH,  $\geq 99\%$ ), potassium hydroxide (KOH, 85 %), hydrochloric acid (HCl, 37 %), sulfuric acid ( $\text{H}_2\text{SO}_4$ , 98 %), diethyl ether ( $(\text{C}_2\text{H}_5)_2\text{O}$ , 99.5 %), hexane ( $\text{C}_6\text{H}_{14}$ , 95 %), methanol ( $\text{CH}_3\text{OH}$ , 99.8 %) and ethanol ( $\text{C}_2\text{H}_5\text{OH}$ ,  $\geq 99.8\%$ ) were purchased from Carlo Erba.

Sunflower oil was purchased from a local market of Aguascalientes (Mexico), while WCO was supplied by GF Energy (Athens, Greece).

### 2.2 Analytical equipments and chemical characterization

A carbolite Eurotherm tubular furnace was used for the pyrolysis of avocado seeds and the synthesis of carbon-based calcium catalysts.

Infrared spectra (FTIR) of synthesized catalysts were recorded by using a Nicolet iS10 Thermo Scientific spectrometer with a resolution of 4 cm<sup>-1</sup>, equipped with a DTGS KBr detector. Prior to the acquisition of FTIR spectra (which was performed in the range of

4000–500  $\text{cm}^{-1}$ ), each sample was mixed with potassium bromide (KBr, FTIR grade) and pressed to obtain pellets, which were utilized in the analysis.

X-ray diffraction (XRD) analysis were performed using an Empyrean (Malvern-Panalytical) diffractometer equipped with a PIXcel1D-Medipix3 detector, operating with  $\text{CuK}\alpha$  radiation ( $\lambda = 1.5406 \text{ \AA}$ , 45 kV, 40 mA). The data were collected in a  $10^\circ < 2\theta < 150^\circ$  range and processed with HighScore Plus software and PDF2 database.

Scanning electron microscopy-energy dispersive X-ray (SEM-EDX) analysis were carried out with FEI Quanta 3D FEG equipment under high vacuum conditions, using secondary electron (SE) and backscattered electron (BSED) detectors. Analyses were performed at 20 kV and a working distance of 9.7 mm.

Organic elemental analysis (C, H, N, S) were carried out with LECO CHNS equipment with oxygen content estimated by difference.

Metals analysis (Ca and other metals) were performed by Wavelength Dispersive X-ray Fluorescence (WDXRF) with a Bruker S8 tiger spectrometer.

Surface areas were measured by nitrogen adsorption at  $-196^\circ\text{C}$  using Quadrasorb Evo equipment.

The Boehm titration method [58] was used for the determination of acid and basic sites of the catalysts.

Identification of the different methyl esters was carried out by gas chromatography-mass spectroscopy (GC-MS) using a Perking Elmer Clarus 500 equipped with a Clarus spectrometer. Quantitative determinations were performed using a Varian 3800 GC-FID. Both instruments were configured for cold on-column injections with a HP-5MS capillary column (30 m;  $\varnothing$  0.32 mm; 0.25  $\mu\text{m}$  film).

Mono-, di- and triglycerides were determined according to the EN14105 procedure (EN14105:2011).

Dissolved calcium was measured by Atomic Absorption Spectroscopy (AAS) with an ICE 3000 Thermo Scientific spectrometer.

### 2.3 *Synthesis of biochar and carbon-based calcium catalysts*

Avocado seeds obtained from the fruit of *Persea Americana* were used as precursors for the synthesis of carbon-based calcium catalysts. Biomass was previously washed with hot deionized water, dried in an oven for 48 h at 105 °C, crashed and sieved (20-40 mesh) [55]. Carbon material (biochar) was obtained by pyrolysis of pre-treated biomass for 2 h at 900 °C with a heating rate of 10 °C min<sup>-1</sup> and a N<sub>2</sub> flow of 100 mL min<sup>-1</sup>. Carbon-based calcium catalysts were synthesized using the precipitation method. 10 g of biochar were suspended in 100 mL of an aqueous solution of Ca(NO<sub>3</sub>)<sub>2</sub>·4H<sub>2</sub>O (11.78 g, weight ratio Ca to biochar of 20%). Then, 66.5 mL of NaOH 1.5 N were added dropwise obtaining the precipitation of calcium hydroxide (Ca(OH)<sub>2</sub>). This suspension was kept under stirring for 1 h at 70 °C. Finally, the resulting solid was filtered, isolated and washed with deionized water (1 L). Subsequently solids were dried and activated for additional 2 h at 900 °C under N<sub>2</sub> flow [41]. The same procedure was used for the preparation of supported catalysts with 10 and 5 wt.% of calcium, using 5.89 and 2.94 g of Ca(NO<sub>3</sub>)<sub>2</sub>·4H<sub>2</sub>O, respectively.

### 2.4 *Transesterification reaction of sunflower oil with methanol*

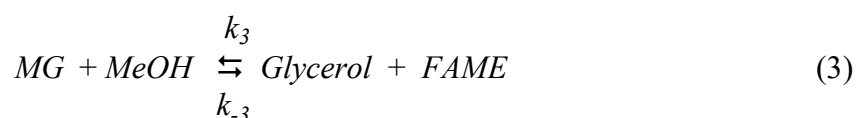
In a Sovirel/Pyrex reactor tube of 15 mL, 2 g of sunflower oil (acidity = 0.21 mg KOH g<sup>-1</sup>, AMW = 280.24 g mol<sup>-1</sup> referred to FFA) were placed with 1.09 g of methanol (molar ratio methanol to oil = 15) and 0.1 g of catalyst (weight ratio catalyst to oil = 5%). Then, a magnetic stirrer was also introduced. The reactor was closed and placed into a thermostatic bath at 100 °C for 3 h under agitation (500 rpm) [59]. It was then



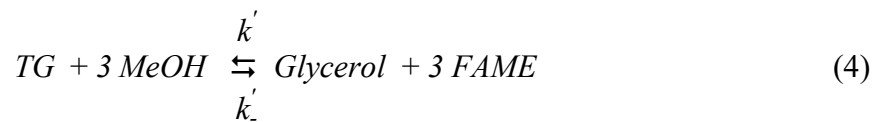
cooled to room temperature and the catalyst was recovered by centrifugation. Methanol was evaporated under N<sub>2</sub> flow, obtaining the separation and decantation of glycerol. The upper organic phase was recovered, washed with deionized water and dried under vacuum. Finally, the content of methyl esters was determined by gas-chromatography using methyl heptadecanoate as an internal standard [60,61]. The effect of the amount of calcium loaded (5, 10 and 20 wt.%) on the surface of the catalysts in the transesterification process was also investigated.

#### *2.4.1 Reaction kinetics for the transesterification process and determination of activation energy*

The transesterification of triglycerides (TG) with methanol is a complex reaction that proceeds in three reversible and consecutive steps [62,63]. TG are converted stepwise to diglycerides (DG), monoglycerides (MG) and finally, to glycerol by obtaining FAME in each step, as shown in Eqs. 1-3:



However, the overall transesterification reaction with the formation of three moles of FAME can also be considered (Eq. 4):



Sunflower oil is mainly made up of triglycerides (> 95 wt.%) and in a small part of DG and MG. For this reason, in order to simplify the kinetic analysis of data, the following assumptions were taken into account [64]: i) the rate constant was determined considering the overall transesterification without intermediate steps (Eq. 4), ii) there was no change in the volume mixture in the liquid phase during the reaction and iii) the high excess of methanol shifted the transesterification equilibrium towards the formation of products and, especially during initial reaction time (60-120 minutes), reverse reaction can be ignored. Consequently, the reaction rate related to the conversion of triglycerides can be expressed by Eq. 5:

$$-\frac{dC_{TG}}{dt} = k' C_{TG}^{\alpha} C_{MeOH}^{\beta} \quad (5)$$

where  $\alpha$  and  $\beta$  are the reaction orders,  $C_{TG}$  and  $C_{MeOH}$  are the concentrations of TG and methanol, respectively, and  $k'$  is an empirical reaction rate. Considering that three moles of methyl esters are obtained for each mole of TG, the concentration of reagents and products ( $C_{FAME}$ ) can be expressed in terms of initial concentration ( $C_{TG0}$ ) and conversion ( $\chi_{TG}$ ) of TG (Eqs. 6 and 7):

$$C_{TG} = C_{TG0}(1 - \chi_{TG}) \quad (6)$$

$$C_{FAME} = 3C_{TG0}\chi_{TG} \quad (7)$$

By substituting Eqs. 6 and 7 into Eq. 5, the following equation was obtained (Eq. 8):

$$-\frac{d\chi_{TG}}{dt} = \frac{k'}{C_{TG0}} C_{TG0}^{\alpha} (1 - \chi_{TG})^{\alpha} C_{MeOH}^{\beta} \quad (8)$$

In the case studied, since methanol is present in great excess compared to TG (molar ratio methanol to oil = 15), its concentration can be considered constant. Therefore,  $C_{MeOH}$  is combined to  $k'$  and  $C_{TGO}^a$  terms, by obtaining the pseudo-reaction rate constant  $k$  (Eq. 9):

$$-\frac{d\chi_{TG}}{dt} = k(1 - \chi_{TG})^\alpha \quad (9)$$

the conversion of TG at time  $t$  ( $\chi_{TG}(t)$ ) was calculated as follows (Eq. 10):

$$\chi_{TG}(t) = \left( \frac{C_{FAME}(t)}{3C_{TGO}} \right) \quad (10)$$

Finally, the activation energy ( $E_a$ ) was obtained by applying the linear form of the Arrhenius equation (Eq. 11):

$$\ln k = \ln A - \frac{E_a}{RT} \quad (11)$$

where  $A$  is a pre-exponential factor and  $R$  is the universal gas constant (8.314 J mol<sup>-1</sup>K<sup>-1</sup>).

#### 2.4.2 Determination of the thermodynamic parameters related to the energy of activation

Using the results of kinetic analysis, the thermodynamic parameters related to the energy of activation including Enthalpy ( $\Delta^\ddagger H$ ), Entropy ( $\Delta^\ddagger S$ ) and Gibbs free energy ( $\Delta^\ddagger G$ ) were also calculated using the Eyring-Polanyi equation (Eq. 12):

$$k = K \frac{k_b T}{h} \exp\left(-\frac{\Delta^\ddagger G}{RT}\right) \quad (12)$$

where  $K$  is the transmission coefficient (which is usually equal to 1 [65]),  $k_b$  is the Boltzmann constant (1.38 x 10<sup>-23</sup> J K<sup>-1</sup>) and  $h$  is the Plank constant (6.63 x 10<sup>-34</sup> J s).

$$\Delta^\ddagger G = \Delta^\ddagger H - T\Delta^\ddagger S \quad (13)$$

By substituting the Gibbs Free Energy equation (Eq. 13) into Eq. 12, the following linear equation can be written (Eq. 14):

$$\ln\left(\frac{k}{T}\right) = -\frac{\Delta^\ddagger H}{RT} + \left[ \ln\left(\frac{k_b}{h}\right) + \frac{\Delta^\ddagger S}{R} \right] \quad (14)$$

where  $\Delta^\ddagger H$  and  $\Delta^\ddagger S$  can be obtained from the slope and the intercept of linear Eyring-Polanyi plot, respectively. Finally,  $\Delta^\ddagger G$  was calculated according to Eq. 13.

#### 2.4.3 Optimization of transesterification conditions

A three-step approach was used to study the effects of the process variables in the conversion of TG into methyl esters and maximization of their yield [66]. Firstly, a three-level and four factorial Box-Behnken experimental design was employed to reduce the number of experiments required for a full factorial design. Molar ratio methanol to oil (5, 10 and 20), catalyst concentration (2.5, 5 and 7.5 wt.% compared to oil), temperature (60, 80 and 100 °C) and reaction time (1, 3 and 5 h) were selected as the independent variables (factors), while FAME content (wt.%) was selected as the dependent variable (response). A total of 27 experiments, including three replicates of the center point, were used for fitting a second-order response surface. The effects of factors on the response were analyzed by using the following quadratic function (Eq. 15):

$$Y = \alpha_0 + \sum_{i=1}^n \alpha_i X_i + \sum \alpha_{ii} X_i^2 + \sum \sum_{i < j}^n \alpha_{ij} X_i X_j \quad (15)$$

where  $Y$  represents the FAME content (wt.%),  $X_i$  and  $X_j$  are the independent variables,  $\alpha_0$ ,  $\alpha_i$ ,  $\alpha_{ij}$  and  $\alpha_{ii}$  are the offset term, linear, interaction and quadratic parameters, respectively. Using the above model, Statgraphycs® Centurion XVI was employed for

the regression analysis and plot response surface. Then, the analysis of variance (ANOVA) significance for the mathematical model describing the functional relationship between factors and the response was performed. The adequacy of the polynomial model to fit experimental data was expressed as  $R^2$  (coefficient of determination) and in its adjusted form. The statistical significance of  $R^2$  was verified by the F-test at a confidence level of 95 %. Finally, the optimization was carried out using Response Surface Methodology (RSM) combined with the desirability function approach to form the desirability optimization methodology (DOM) [67].

#### 2.4.4 *Recyclability of supported catalyst in the transesterification reaction*

The recyclability of the catalyst was tested in the transesterification of sunflower oil with methanol. At the end of a reaction cycle, the catalyst was recovered by centrifugation and directly re-used with fresh sunflower oil and methanol for a new reaction run. Alternatively, the recovered catalyst, was first washed with methanol, dried at 100 °C for 3 h and re-activated at 550 °C for 2 h under N<sub>2</sub> flow before its reuse. Recyclability was tested two times and the respective FAME content of the resulting products was determined. In addition, the leaching of Ca after each reaction cycle was evaluated by AAS on mineralized sample of final products.

#### 2.5 *Transesterification reaction of pre-treated waste cooking oil*

A two-step process of direct esterification and basic transesterification reaction was adopted for the conversion of a real sample of WCO into biodiesel. In detail, the direct esterification of FFA into the corresponding methyl esters was operated by using AlCl<sub>3</sub>·6H<sub>2</sub>O as catalyst. Reaction conditions reported by di Bitonto and Pastore [57] were used. Namely, 100 g of WCO were reacted at 70 °C for 4 h with 100 g of MeOH

and 0.242 g of  $\text{AlCl}_3 \cdot 6\text{H}_2\text{O}$ . A biphasic system was obtained. Then, 5 g of the oily layer (pre-treated WCO) was directly used in the transesterification process. The reaction was carried out at 99.5 °C for 5 h using 7.3 wt.% of supported catalyst with 20 wt.% of Ca loaded (compared to the starting oil) and a molar ratio methanol to pre-treated oil was corrected to 15.6 by adding methanol. For the kinetic study, samples (0.3 mL) were collected at 1, 2, 3, 4 and 5 h of reaction, processed (see Section 2.3) and analyzed for the determination of FAME and glycerides content.

### 3. Analysis of results

#### 3.1 *Synthesis and characterization of carbon-based calcium catalysts*

Avocado seeds were used as the initial raw material for preparing biochar through a thermal treatment under nitrogen flow (900 °C, 2 h). The initial avocado seeds were mainly constituted by (dry composition): simple sugars (4-6 wt.%), easily hydrolyzable sugars (EHS, 48-50 wt.%), lignin (4-6 wt.%), lipids (3-5 wt.%), proteins (2-4 wt.%), cellulose (1-2 wt.%) and ashes (1-2 wt.%) [68]. In addition, they contain some polyphenolic compounds such as tannins, catechins, flavonols and anthocyanins [69]. As a result of the carbonization process, gas and liquid phases were also produced during pyrolysis. Gas phase was mainly composed by  $\text{H}_2$ , CO,  $\text{CO}_2$  and  $\text{CH}_4$  [70], while liquid phase (also known as tar) was composed by acids, alcohols, ketones, phenols, sugars, furans, esters, aldehydes, among others [70,71]. These pyrolysis sub-products could be utilized for the production of a wide variety of chemicals as well as alternative fuels for heat and electricity generation [70,72].

Preliminary studies indicated that surface area of biochar increased mainly with pyrolysis temperature. In fact, thermogravimetric analyses of several lignocellulosic biomasses indicated that the volatile matter is removed thus favoring pore formation

when biomass pyrolysis is performed at  $> 600\text{ }^{\circ}\text{C}$ . In this study, a high pyrolysis temperature ( $900\text{ }^{\circ}\text{C}$ ) was adopted, in order to obtain a good tradeoff between porosity and surface chemistry of the biochar with the objective to achieve an effective anchoring of catalytic phase (i.e., calcium). Note that several authors have established that high catalytic activity is not always related to high surface areas, where the surface chemistry is more important than textural parameters [73]. Regarding biochar, an organic material characterized by a low oxygen content was obtained (E1, Table 1), due to the partial loss of primary hydroxyl groups present on the surface with the formation of ether bonds [74]. Nitrogen and sulfur were also present (1.99 and 0.95 wt.%, respectively), for the partial decomposition of amino acids and other nitrogen compounds [75]. The synthetic procedure for the preparation of carbon-based calcium catalysts consisted in the direct titration with NaOH of aqueous solutions of calcium nitrate at different concentrations, in which the biochar was also suspended. Next, the solids were recovered by filtration, washed with deionized water and activated for 2 h at  $900\text{ }^{\circ}\text{C}$  under  $\text{N}_2$  flow. The effect of Ca loaded on the structure and the chemical properties of synthesized catalysts were investigated and compared with the native biochar obtained by pyrolysis of dried biomass: elemental analysis, FTIR, XRD, SEM, BET surface area, acid and basic sites were carried out.

*Please Insert Table 1*

The precipitation method efficiently allowed to deposit calcium on the surface of the chars (E2-4, Table 1). Increasing the amount of Ca loaded from 5 to 20 wt.% (compared to biochar), an increase of Ca content was observed from 2.26 to 12.0 wt.%, respectively.

*Please Insert Fig. 1*

FTIR analysis also provided important information on the structure of these systems (Fig. 1a). A broad band at  $3435\text{ cm}^{-1}$  was detected in all synthesized samples, which can be attributed to the stretching signals of  $\text{-OH}$  and  $\text{-NH}$  groups [76]. Signals located at  $2960$  and  $2920\text{ cm}^{-1}$  correspond instead to the stretching signals of aliphatic structures. FTIR spectrum of biochar showed a typical band at  $1620\text{ cm}^{-1}$ , associated to  $\text{C}=\text{C}$  stretching of polynuclear aromatic compounds and signals located at  $1120$ ,  $1088$  and  $1056\text{ cm}^{-1}$  assigned to  $\text{C-O}$  stretching of tertiary, secondary and primary hydroxyl groups, respectively [77]. FTIR spectra of the carbon-based calcium catalysts showed additional bands which could be associated to the presence of Ca on the surface. The sharp stretching band at  $3644\text{ cm}^{-1}$  was assigned to the structural hydroxyl groups of  $\text{Ca(OH)}_2$  as reported in literature [43]. In addition, particularly evident is the presence of a broad band at  $1420\text{ cm}^{-1}$  and signals located at  $873$  and  $714\text{ cm}^{-1}$  (absent in synthesized biochar) which were attributed to asymmetric stretch, out-of plane bend and in plane bend vibration modes, respectively, for calcium carbonate  $\text{Ca(CO)}_3$ , obtained by a partial carbonation of  $\text{CaO}$  [78]. As result, XRD analysis (Fig. 1b) displayed the presence of  $\text{CaO}$  crystallites, identified by well-resolved diffraction peaks  $2\theta$  at:  $32.18^\circ$ ,  $37.32^\circ$ ,  $53.82^\circ$ ,  $64.11^\circ$ ,  $67.32^\circ$ ,  $79.61^\circ$  and  $88.46^\circ$  [79] and with the intensity of signals proportional to the amount of Ca loading.

*Please Insert Fig. 2*

SEM analysis showed significant differences among the surface morphology of the investigated catalysts (Fig. 2). Biochar (Fig. 2a) presents an alveolar structure characterized by an assorted pore size, in which a narrow mesoporosity predominates (E1, Table 2). Such morphology obtained as a result of the release of volatile compounds during thermal treatment, favors the deposition and the anchoring of calcium since it is a small ion. In comparison with Figs. 2b-d, it was possible to observe



how nanostructures of CaO covered the pores of carbonized support quite uniformly, leaving behind a porous surface with a large number of micropores (E4, Table 2). As result, we observed a progressive increase of the BET surface area and basic properties for carbon-based calcium catalysts (see Fig. 3b).

*Please Insert Table 2*

### 3.2 *Transesterification tests for biodiesel production: effect of calcium loaded on catalyst activity*

Preliminary tests were conducted on sunflower oil to test the efficacy of synthesized catalysts in biodiesel production and compared with CaO. The reaction was carried out at 100 °C for 3 h, by using the experimental conditions described in Section 2.4. At the end of the reaction, the upper organic phase was recovered and analyzed for the determination of FAME content. The results obtained are reported in Fig. 3a.

*Please Insert Fig. 3*

CaO showed a high activity in the transesterification reaction (FAME content = 87.1 wt.%), but a large part of the catalyst was lost during the reaction due to the dissolution of metal oxide in the reaction medium, producing a homogeneous catalytic activity [39,40]. Conversely, the native biochar revealed a very low activity (FAME content = 0.76 wt.%). Concerning the supported catalysts, with the increase of the amount of Ca loaded from 5 to 20 wt.%, an increase of FAME content was observed, strictly connected to the basic properties of the catalysts (Fig. 3b). This is due to the preparation method, based on the precipitation followed by the subsequent heat treatment (900 °C, 2 h), which led to a partial inclusion and agglomeration phenomena of CaO, onto the alveolar structure of the support, limiting the effective availability of final active basic

sites (Fig. 2). In the case of Ca loaded with 20 wt.%, a FAME content of 82.7 wt.% was achieved. In addition, when compared to the use of CaO, the supported catalysts were easily recovered and re-used for several cycles without a significant loss of catalytic activity (see Section 3.6).

### 3.3 *Effects of temperature and reaction time*

Once the supported catalyst loaded with 20 wt.% of Ca had been identified as the most active catalyst in transesterification reaction of sunflower oil with methanol, the effects of temperature and reaction time were also investigated by using a catalytic system of this type. Reaction kinetics were carried out at different temperatures (60, 80 and 100 °C) at a molar ratio methanol to oil of 15 and a weight ratio catalyst to oil of 5 wt.%. The results obtained are reported in Fig. 4a.

*Please Insert Fig. 4*

The reaction time had a significant effect in the transesterification process. Extending the reaction time up to 5 h at 100 °C, a further increase of FAME content up to 91.1 wt.% was achieved in the isolated products. Instead, the decrease of temperature drastically reduced the reaction rate and the final conversion into methyl esters: FAME content of 43.5 and 70 wt.%, were respectively obtained at 60 and 80 °C, after 5 h of reaction. Based on these results, the pseudo-first order and the pseudo-second order models were used to fit the experimental data in function of reaction time (Figs. 4b-c). Kinetic parameters obtained by using these two models and related coefficients of determination ( $R^2$ ) are reported in Table 3.

*Please Insert Table 3*

The pseudo-second order kinetic model was the most appropriate to fit the experimental data.  $A$  and  $E_a$  were then calculated by plotting the logarithm of the rate constants ( $k$ ) versus  $1/T$  (Fig. 5).

*Please Insert Fig. 5*

The experimental  $E_a$  value was 39.9 kJ mol<sup>-1</sup>. The activation energy for the transesterification process of vegetable oils with methanol by using homogeneous alkaline catalysts (acidity < 1.5 wt.%) is usually 20-30 kJ mol<sup>-1</sup>, while for several heterogeneous catalysts  $E_a$  ranged between 40 and 130 kJ mol<sup>-1</sup> (see Table 4). According to these data, 20 wt.% of Ca loaded onto avocado char, resulted as more active than ionic liquids (E3-5) or other heterogeneous systems (E6-10), confirming the efficacy of the catalyst in the process.

*Please Insert Table 4*

### 3.4 Determination of the thermodynamic parameters related to the energy of activation

Finally, thermodynamic parameters ( $\Delta^\ddagger H$ ,  $\Delta^\ddagger S$  and  $\Delta^\ddagger G$ ) related to the energy of activation (transition state) of the transesterification reaction catalyzed by supported catalyst loaded with 20 wt.% of Ca were calculated using the Eyring–Polanyi equation (Fig. 6).

*Please Insert Fig. 6*

*Please Insert Table 5*

The process was found to be non-spontaneous, with the values of  $\Delta^\ddagger H$  (37.05 kJ mol<sup>-1</sup>) and  $\Delta^\ddagger G$  calculated at different temperatures (98.68-106.08 kJ mol<sup>-1</sup>) which both

resulted positive. Instead, the negative value of  $\Delta^\ddagger S$  ( $-0.185 \text{ kJ mol}^{-1} \text{ K}$ ) indicated how the transition state has a higher degree of order geometry than the ground state reactants. As a consequence, heat input is required to bring the reagents to the transition state and lead to the formation of the final products.

### 3.5 Analysis of optimum conditions

In order to maximize the FAME content in the organic phase isolated at the end of the process, the optimization of reaction conditions was conducted by response surface methodology of a Box-Behnken factorial design of experiments (Table 6). Molar ratio methanol to oil ( $mol$ ), catalyst concentration ( $cat$ ), temperature ( $T$ ) and reaction time ( $t$ ) were selected as factors while FAME content ( $wt.\%$ ) was selected as response. A quadratic regression model was used to fit the experimental data, by obtaining the following relationship between factors and response (Eq. 16):

$$\begin{aligned} \text{FAME content (wt.\%)} = & -162.71 + 4.50325mol + 4.46733cat + 1.82206T + 7.69187t + \\ & 0.00551667mol^2 - 0.230933cat^2 - 0.00518333T^2 - 2.97052t^2 + -0.139 molcat \\ & - 0.03785molT + 0.40475molt + 0.0362 catT + 1.156 catt + 0.131688 Tt \end{aligned} \quad (16)$$

*Please Insert Table 6*

Subsequently, the statistical analysis of the estimated effects for the adopted model was performed by the analysis of variance (ANOVA). The significance of the mathematical model was associated to the P-value. In this case, a value of 0.05 was considered as a suitable threshold with the corresponding significant parameters which were highlighted with an asterisk. The main statistics associated to the model and the different components of the fitting equation are reported in Table 7.

*Please Insert Table 7*

All linear parameters were significant in the transesterification reaction of sunflower oil with methanol. Reaction time showed the most significant effect followed by temperature, catalyst concentration and methanol, respectively. Concerning the other terms, only *catt* (the interaction between catalyst concentration and time), *Tt* (the interaction between temperature and time) and  $t^2$  (the quadratic term associated with the temperature) were significant. The efficacy of the model was then evaluated by using the coefficient of determination  $R^2$ . The value obtained of 0.9776, in its adjusted form, indicates a high reliability of the model used.

*Please Insert Fig. 7*

Finally, the response surface plots were generated in order to identify the optimal experimental conditions required for the complete conversion of the starting oil into FAME. Fig. 7a shows the combined effect of temperature and reaction time, with a fixed catalyst concentration of 5 wt.% and molar ratio methanol to oil of 10. With the increase of temperature and reaction time, an increase of FAME content in the product isolated was observed, up to obtaining a value close to 95 wt.% at 100 °C after 5 h of reaction. A similar effect was detected in Fig. 7b in which the effect of the catalyst concentration in relation to temperature was also investigated (molar ratio methanol to oil = 10, time = 3 h). Fig. 7c and 7d show the combined effects of molar ratio methanol to oil and reaction time (catalyst = 5 wt.%) and catalyst concentration and molar ratio methanol to oil (time = 3 h), maintaining a fixed temperature of 80 °C, respectively. In both cases, a clear kinetic limit was observed with a maximum FAME content of 80 wt.%. At the end of this study, the optimal conditions were determined and directly applied in the transesterification of sunflower oil with methanol. A biodiesel with methyl esters content of  $99.5 \pm 0.3$  wt.% was obtained at 99.5 °C after 5 h of reaction

with a molar ratio MeOH to oil of 15.6 and catalyst concentration of 7.3 wt.%. The produced biodiesel was found to fulfill EN14214 specifications.

### 3.6 *Recovery and reuse of the catalyst*

One of the major problems related to the use of calcium-based heterogeneous catalysts and which provides important information about their stability is the leaching of Ca from the catalyst into the reaction medium. For this reason, the reusability of a supported catalyst with 20 wt.% of Ca loaded was evaluated, by operating batch runs for three consecutive times under optimal reaction conditions (molar ratio methanol to oil = 15.6, weight ratio catalyst to oil = 7.3 %, 99.5 °C, 5 h). After each reaction cycle, the catalyst was recovered by centrifugation and used directly in a new reaction cycle using fresh methanol and oil, without any further treatments. The results are reported in Fig. 8.

*Please Insert Fig. 8*

The FAME content of the products isolated were 99.5, 90 and 80 wt.%, respectively. The slight decrease of the catalytic activity may be due to two possible causes: i) the partial dissolution and loosing of the calcium catalyst in the reaction medium or ii) the reduction of the active sites on the surface of the catalyst due to the deposition of organic molecules deriving from the reaction mixture. The leaching of calcium was determined through AAS analysis after each cycle of reuse. It was observed that the amount of calcium leached clearly decreased from the first (11.5 mg) to the second cycle (4.9 mg), up to disappearing completely in the third cycle. The contribution to the homogeneous catalysis of the transesterification reaction, due to the soluble calcium dissolved after leaching, was determined by testing the reactivity of an equivalent amount of CaO (16.1 mg) with sunflower oil and methanol under the same experimental conditions. At the end of this test, CaO was completely dissolved and a FAME yield of

31.4 wt.% was finally achieved. Therefore, the contribution of the homogeneous species created by leaching results as negligible with the catalysis that occurred mainly on the surface of the catalyst. XRD spectrum of supported catalyst recovered at the end of third cycle of reaction, showed significant changes in the surface texture (see Fig. 9a). CaO peaks observed in the starting sample were absent with the formation of  $\text{Ca}(\text{OH})_2$ . New signals were detected at  $2\theta$  of  $20.17^\circ$ ,  $23.42^\circ$ ,  $27.46^\circ$ ,  $31.23^\circ$ ,  $36.35^\circ$  and  $42.29^\circ$ , attributable to the deposition of organic molecules on the surface of the catalyst. Such a hypothesis was also confirmed by FTIR analysis (Fig. 9b): the intensive doublet located at 2930 and  $2860\text{ cm}^{-1}$ , associated to C-H stretching of methyl and methylene groups and the signal located at  $1744\text{ cm}^{-1}$  (C=O stretching of carbonyl groups) were associated to the presence of FAME and other organic products (glycerol, mono- and diglycerides) deriving from the transesterification process. Therefore, the organic molecules deposited on the catalyst surface lead to a reduction of its catalytic activity, by leading to a low accessibility of the active sites. To resolve this problem, the catalyst recovered at each reaction cycle was washed with methanol, dried in an oven at  $100^\circ\text{C}$  for 3 h and then reactivated at  $550^\circ\text{C}$  for 2 h under  $\text{N}_2$  flow [79]. When the catalyst was reused for other three cycles of reaction, it totally restored and maintained its catalytic activity. In addition, the leaching content in the isolated biodiesel was remarkably low ( $<1\text{ ppm}$ ), confirming the stability and lifetime of the catalyst.

### 3.7 *Conversion of waste cooking oil into biodiesel*

The use of non-edible oils represents a useful way to produce biodiesel not only in order to reduce its manufacturing costs, but also for ethical and environmental concerns. The most commonly adopted strategy for the conversion of raw oils (FFAs content 1-90 wt.%) is a two-step procedure in which generally an acid catalyst was first used for the

direct esterification of FFAs as a pre-treatment and subsequently, a basic catalyst was added for the transesterification of glycerides. Consequently, a supported catalyst with 20 wt.% of Ca loaded was finally tested for the transesterification of pretreated WCO. A real sample of WCO was in fact reacted with methanol in presence of  $\text{AlCl}_3 \cdot 6\text{H}_2\text{O}$  [57].  $\text{AlCl}_3 \cdot 6\text{H}_2\text{O}$  was chosen instead of  $\text{H}_2\text{SO}_4$ , because it allowed the direct esterification reaction of FFAs and methanol to be promoted in a homogenous phase. The reaction resulted fast and complete as when  $\text{H}_2\text{SO}_4$  was used. In addition, several further advantages were achieved.  $\text{AlCl}_3 \cdot 6\text{H}_2\text{O}$  did not need the use of expensive materials for reactors and pipelines because it is less aggressive than conventional mineral acids. Differently from  $\text{H}_2\text{SO}_4$ , it was easily and completely recovered at the end of reaction. In fact, after the pretreatment, a biphasic system was finally obtained: an upper methanol phase, in which most of water produced by direct esterification and most of catalyst were dissolved, and a bottom oily layer containing most of the FAME and glycerides. Methanol layer phase can be even directly reused for several new cycles of pretreatments of WCO, without generating any salty-waste [57].

*Please Insert Table 8*

As shown in Table 8, after the direct esterification process, the acidity of the pretreated WCO (oily phase) decreased from 8.05 to 0.77 mg KOH g<sup>-1</sup> due to the selective conversion of FFAs into methyl esters (FAME content = 4.4 wt.%). MG were absent, while the contents of DG and TG were 5.6 and 89.2 wt.%, respectively. The oily layer was then directly reacted with methanol and 20 wt.% calcium deposited avocado char as a catalyst, under optimized conditions as described in the Section 3.5. Results are reported in Fig. 10. The reaction was already completed after 2 h, isolating at the end a biodiesel compliant with EN14214 specifications (Table 9).

*Please Insert Table 9*



In addition, compared to the use of homogenous basic catalysts (NaOH, KOH), the separation of the catalyst was easily achieved through centrifugation, and even the recovery of biodiesel from the glycerol phase occurred easily and without any emulsions, confirming the efficacy of the entire process.

*Please Insert Fig. 10*

#### 4. Conclusions

In this work nanostructured calcium oxide deposited onto biochar deriving from avocado seeds was synthesized, characterized and tested in the transesterification reaction of sunflower oil with methanol. The catalysts were synthesized by the coprecipitation method, varying the amount of initial Ca loaded. After a thermal treatment (900 °C, 2 h, N<sub>2</sub> flow), CaO was obtained and homogeneously dispersed onto the surface of carbonized supports. Spectroscopy techniques and elemental analysis confirmed the presence of CaO nanoparticles uniformly dispersed and anchored onto the alveolar structure of the support. The increase of calcium oxide content positively affected the basicity and consequently the catalytic activity in transesterification of glycerides. In fact, supported catalyst with 20 wt.% of Ca loaded showed the best catalytic activity in the transesterification process. In addition, compared to the use of CaO, the catalyst was easily recovered by centrifugation, regenerated (through a thermal treatment, 550 °C, 3 h, under N<sub>2</sub> flow) and reused for three cycles of reaction without any significant loss of activity. The transesterification reaction followed the pseudo-second order kinetic model with an  $E_a$  value of 39.9 kJ mol<sup>-1</sup>. This indicated that the catalytic performance of supported catalyst with 20 wt.% of Ca loaded is better than the use of ionic liquids and other heterogeneous systems. Then, a response surface methodology was applied to investigate the optimum conditions and maximize the

production of FAME. At 99.5 °C after 5 h, a FAME content of 99.5% was achieved by using a molar ratio methanol to oil of 15.6 and 7.3 wt.% of catalyst. Finally, the optimized conditions were positively tested in the transesterification of pretreated WCO after a preliminary conversion of FFAs into methyl esters using  $\text{AlCl}_3 \cdot 6\text{H}_2\text{O}$  as catalyst. Biodiesel isolated at the end of the process was conform to EN14214 standards. These results confirm the efficiency of the entire process and open up the possibility for the application of this technology for the conversion of a number of low quality feedstocks.

### ***Acknowledgments***

This work was supported by IProPBio "Integrated Process and Product Design for Sustainable Biorefineries (MSCA – RISE 2017: Research and Innovation Staff Exchange", Project ID: 778168 and Junta de Extremadura (IB16167).

### **References**

- [1] M.J. Burke, J.C. Stephens, Political power and renewable energy futures: A critical review, *Energ. Res. Soc. Sci.* 35 (2018) 78–93.  
<https://doi.org/10.1016/j.erss.2017.10.018>.
- [2] M.F Demirbas, Biorefineries for biofuel upgrading: a critical review, *Appl. Energ.* 86 (2009) S151–S161. <https://doi.org/10.1016/j.apenergy.2009.04.043>.
- [3] P. Tamilselvan, N. Nallusamy, S. Rajkumar, A comprehensive review on performance, combustion and emission characteristics of biodiesel fuelled diesel engines, *Renew. Sust. Energ. Rev.* 79 (2017) 1134–1159.  
<https://doi.org/10.1016/j.rser.2017.05.176>.

- [4] Y. Huang, Y. Li, X. Han, J. Zhang, K. Luo, S. Yang, J. Wang, Investigation on fuel properties and engine performance of the extraction phase liquid of bio-oil/biodiesel blends, *Renew. Energ.* 147 (2020) 1990–2002.  
<https://doi.org/10.1016/j.renene.2019.10.028>.
- [5] V.B. Borugadda, V.V. Goud, Biodiesel production from renewable feedstocks: Status and opportunities, *Renew. Sust. Energ. Rev.* 16 (2012) 4763–4784.  
<https://doi.org/10.1016/j.rser.2012.04.010>.
- [6] O.M. Ali, R. Mamat, N.R. Abdullah, A.A. Abdullah, Analysis of blended fuel properties and engine performance with palm biodiesel–diesel blended fuel, 86 (2016) 59–67.  
<https://doi.org/10.1016/j.renene.2015.07.103>.
- [7] K.A. Sorate, P.V. Bhale, Biodiesel properties and automotive system compatibility issues, *Renew. Sust. Energ. Rev.* 41 (2015) 777–798.  
<https://doi.org/10.1016/j.rser.2014.08.079>.
- [8] E. Buyukkaya, Effects of biodiesel on a DI diesel engine performance, emission and combustion characteristics, *Fuel* 89 (2010) 3099–3105.  
<https://doi.org/10.1016/j.fuel.2010.05.034>.
- [9] G. Baskar, R. Aiswarya, Trends in catalytic production of biodiesel from various feedstocks, *Renew. Sust. Energ. Rev.* 57 (2016) 496–504.  
<https://doi.org/10.1016/j.rser.2015.12.101>.
- [10] M. Tubino, J.G.R. Junior, G.F. Bauerfeldt, Biodiesel synthesis: A study of the triglyceride methanolysis reaction with alkaline catalysts, *Catal. Comm.* 75 (2016) 6–12. <https://doi.org/10.1016/j.catcom.2015.10.033>.
- [11] V.C. Eze, A.N. Phan, A.P. Harvey, Intensified one-step biodiesel production from high water and free fatty acid waste cooking oils, *Fuel* 220 (2018) 567–574. <https://doi.org/10.1016/j.fuel.2018.02.050>.

- [12] P. Verma, M.P. Sharma, Review of process parameters for biodiesel production from different feedstocks, *Renew. Sust. Energ. Rev.* 62 (2016) 1063–1071.  
<https://doi.org/10.1016/j.rser.2016.04.054>.
- [13] J. Marchetti, A. Errazu, Esterification of free fatty acids using sulfuric acid as catalyst in the presence of triglycerides, *Biomass Bioenerg.* 32 (2008) 892–895.  
<https://doi.org/10.1016/j.biombioe.2008.01.001>.
- [14] M. Di Serio, R. Tesser, M. Dimiccoli, F. Cammarota, M. Nastasi, E. Santacesaria, Synthesis of biodiesel via homogeneous Lewis acid catalyst, *J. Mol. Catal. A: Chem* 239 (2005) 111–115.  
<https://doi.org/10.1016/j.molcata.2005.05.041>.
- [15] P. Andreo-Martínez, V.M. Ortiz-Martínez, N. García-Martínez, A.P. de los Ríos, F.J. Hernández-Fernández, J. Quesada-Medina, Production of biodiesel under supercritical conditions: State of the art and bibliometric analysis, *Appl. Energ.* 264 (2020) 114753. <https://doi.org/10.1016/j.apenergy.2020.114753>.
- [16] R. Alenezi, G.A. Leeke, J.M. Winterbottom, R.C.D. Santos, A.R. Khan, Esterification kinetics of free fatty acids with supercritical methanol for biodiesel production, *Energ. Convers. Manage.* 51 (2010) 1055–1059.  
<https://doi.org/10.1016/j.enconman.2009.12.009>.
- [17] C. Mueanmas, R. Nikhom, A. Petchkaew, J. Iewkittayakorn, K. Prasertsit, Extraction and esterification of waste coffee grounds oil as non-edible feedstock for biodiesel production, *Renew. Energ.* 133 (2019) 1414–1425.  
<https://doi.org/10.1016/j.renene.2018.08.102>.
- [18] M.E. Borges, L. Díaz, Recent developments on heterogeneous catalysts for biodiesel production by oil esterification and transesterification reactions: a review, *Renew. Sust. Energ. Rev.* 16 (2016) 2839–2849.  
<https://doi.org/10.1016/j.rser.2012.01.071>.

- [19] R. Malhotra, A. Ali, 5-Na/ZnO doped mesoporous silica as reusable solid catalyst for biodiesel production via transesterification of virgin cottonseed oil, *Renew. Energ.* 133 (2019) 606–619.  
<https://doi.org/10.1016/j.renene.2018.10.055>.
- [20] A.K. Endalew, Y. Kiros, R. Zanzi, Inorganic heterogeneous catalysts for biodiesel production from vegetable oils, *Biomass Bioenerg* 35 (2011) 3787–3809. <https://doi.org/10.1016/j.biombioe.2011.06.011>.
- [21] A. Dibenedetto, A. Angelini, A. Colucci, L. di Bitonto, C. Pastore, C. Giannini, B.M. Aresta, R. Comparelli, Tunable Mixed Oxides: Efficient Agents for the Simultaneous Transesterification of Lipids and Esterification of Free Fatty Acids from Bio-Oils for the Effective Production of Fames, *Int. J. Renew. Energ. Biofuel* (2016) Article ID:204112.
- [22] S. Semwal, A.K. Arora, R.P. Badoni, D.K. Tuli, Biodiesel production using heterogeneous catalysts, *Bioresour. Technol.* 102 (2011) 2151–2161.  
<https://doi.org/10.1016/j.biortech.2010.10.080>.
- [23] J.F. Gomes, J.F. Puna, L.M. Gonçalves, J.C. Bordado, Study on the use of MgAl hydrotalcites as solid heterogeneous catalysts for biodiesel production, *Energy* 36 (2011) 6770–6778. <https://doi.org/10.1016/j.energy.2011.10.024>.
- [24] C.C. Silva, N.F. Ribeiro, M.M. Souza, D.A. Aranda, Biodiesel production from soybean oil and methanol using hydrotalcites as catalyst, *Fuel Process. Technol.* 91 (2010) 205–210. <https://doi.org/10.1016/j.fuproc.2009.09.019>.
- [25] J. Fu, L. Chen, P. Lv, L. Yang, Z. Yuan, Free fatty acids esterification for biodiesel production using self-synthesized macroporous cation exchange resin as solid acid catalyst, *Fuel* 154 (2015) 1–8.  
<https://doi.org/10.1016/j.fuel.2015.03.048>.

- [26] Y. Feng, B. He, Y. Cao, J. Li, M. Liu, F. Yan, X. Liang, Biodiesel production using cation-exchange resin as heterogeneous catalyst, *Bioresour Technol* 101 (2010) 1518–1521. <https://doi.org/10.1016/j.biortech.2009.07.084>.
- [27] A.M. Doyle, T.M. Albayati, A.S. Abbas, Z.T Alismaeel, Biodiesel production by esterification of oleic acid over zeolite Y prepared from kaolin, *Renew. Energ.* 97 (2016) 19–23. <https://doi.org/10.1016/j.renene.2016.05.067>.
- [28] J. Alcañiz-Monge, B. El Bakkali, G. Trautwein, S. Reinoso, Zirconia-supported tungstophosphoric heteropolyacid as heterogeneous acid catalyst for biodiesel production, *Appl. Catal. B: Environ.* 224 (2018) 194–203. <https://doi.org/10.1016/j.apcatb.2017.10.066>.
- [29] J. Gardy, A. Hassanpour, X. Lai, M.H. Ahmed, M. Rehan, Biodiesel production from used cooking oil using a novel surface functionalised TiO<sub>2</sub> nano-catalyst, *Appl. Catal. B: Environ.* 207 (2017) 297–310. <http://dx.doi.org/10.1016/j.apcatb.2017.01.080>.
- [30] J. Gardy, A. Osatiashtiani, O. Céspedes, A. Hassanpour, X. Lai, A.F. Lee, K. Wilson, M. Rehan, A magnetically separable SO<sub>4</sub>/Fe-Al-TiO<sub>2</sub> solid acid catalyst for biodiesel production from waste cooking oil, *Appl. Catal. B: Environ.* 234 (2018) 268–278. <https://doi.org/10.1016/j.apcatb.2018.04.046>.
- [31] Y. Jeon, W.S. Chi, J. Hwang, D.H. Kim, J.H. Kim, Y.G. Shul, Core-shell nanostructured heteropoly acid-functionalized metal-organic frameworks: Bifunctional heterogeneous catalyst for efficient biodiesel production, *Appl. Catal. B: Environ.* 242 (2019) 51–59. <https://doi.org/10.1016/j.apcatb.2018.09.071>
- [32] J. Gardy, E. Nourafkan, A. Osatiashtiani, A.F. Lee, K. Wilson, A. Hassanpour, X. Lai, A core-shell SO<sub>4</sub>/Mg-Al-Fe<sub>3</sub>O<sub>4</sub> catalyst for biodiesel production, *Appl. Catal. B: Environ.* 259 (2019) 118093.

<https://doi.org/10.1016/j.apcatb.2019.118093>.

- [33] L.M. Correia, R.M.A. Saboya, N. de Sousa Campelo, J.A. Cecilia, E. Rodríguez-Castellón, C.L. Cavalcante, R.S. Vieira, Characterization of calcium oxide catalysts from natural sources and their application in the transesterification of sunflower oil, *Bioresour. Technol.* 151 (2014) 207–213.  
<https://doi.org/10.1016/j.biortech.2013.10.046>.
- [34] R. Risso, P. Ferraz, S. Meireles, I. Fonseca, J. Vital, Highly active CaO catalysts from waste shells of egg, oyster and clam for biodiesel production, *Appl. Catal. A: Gen.* 567 (2018) 56–64. <https://doi.org/10.1016/j.apcata.2018.09.003>.
- [35] P.L. Boey, G.P. Maniam, S.A. Hamid, Performance of calcium oxide as a heterogeneous catalyst in biodiesel production: a review, *Chem. Eng. J.* 168 (2011) 15–22. <https://doi.org/10.1016/j.cej.2011.01.009>.
- [36] D.M. Marinković, M.V. Stanković, A.V. Veličković, J.M. Avramović, M.R. Miladinović, O.O. Stamenković, V.B. Veljković, D.M. Jovanović, Calcium oxide as a promising heterogeneous catalyst for biodiesel production: current state and perspectives, *Renew. Sust. Energ. Rev.* 56 (2016) 1387–1408.  
<https://doi.org/10.1016/j.rser.2015.12.007>.
- [37] X. Liu, H. He, Y. Wang, S. Zhu, X. Piao, Transesterification of soybean oil to biodiesel using CaO as a solid base catalyst, *Fuel* 87 (2008) 216–221.  
<https://doi.org/10.1016/j.fuel.2007.04.013>.
- [38] E. Viola, A. Blasi, V. Valerio, I. Guidi, F. Zimbardi, G. Braccio, G. Giordano, Biodiesel from fried vegetable oils via transesterification by heterogenous catalysis. *Catal. Today* 179 (2012) 185–190.  
<https://doi.org/10.1016/j.cattod.2011.08.050>.

- [39] I. Sádaba, M.L. Granados, A. Riisager, E. Taarning, Deactivation of solid catalysts in liquid media: the case of leaching of active sites in biomass conversion reactions, *Green Chem.* 17 (2015) 4133–4145.  
<https://doi.org/10.1039/C5GC00804B>.
- [40] M.L. Granados, D.M. Alonso, I. Sádaba, R. Mariscal, P. Ocón, Leaching and homogeneous contribution in liquid phase reaction catalysed by solids: the case of triglycerides methanolysis using CaO, *Appl. Catal. B: Environ.* 89 (2009) 265–272. <https://doi.org/10.1016/j.apcatb.2009.02.014>.
- [41] M. Kouzu, T. Kasuno, M. Tajika, Y. Sugimoto, S. Yamanaka, J. Hidaka, Calcium oxide as a solid base catalyst for transesterification of soybean oil and its application to biodiesel production, *Fuel* 87 (2008) 2798–2806.  
<https://doi.org/10.1016/j.fuel.2007.10.019>.
- [42] A.P.S. Dias, J. Puna, M.J.N. Correia, I. Nogueira, J. Gomes, J. Bordado, Effect of the oil acidity on the methanolysis performances of lime catalyst biodiesel from waste frying oils (WFO), *Fuel Process Technol* 116 (2013) 94–100.  
<https://doi.org/10.1016/j.fuproc.2013.05.002>.
- [43] M.L. Granados, M.Z. Poves, D.M. Alonso, R. Mariscal, F.C. Galisteo, R. Moreno-Tost, J. Santamaria, J.L.G. Fierro, Biodiesel from sunflower oil by using activated calcium oxide, *Appl. Catal. B: Environ.* 73 (2007) 317–326.  
<https://doi.org/10.1016/j.apcatb.2006.12.017>.
- [44] M.D. Kostic, A. Bazargan, O.S. Stamenkovic, V.B. Veljkovic, G. McKay, Optimization and kinetics of sunflower oil methanolysis catalyzed by calcium oxide-based catalyst derived from palm kernel shell biochar, *Fuel* 163 (2016) 304–313. <http://dx.doi.org/10.1016/j.fuel.2015.09.042>



- [45] S. Wang, R. Shan, Y. Wang, L. Lu, H. Yuan, Synthesis of calcium materials in biochar matrix as a highly stable catalyst for biodiesel production, *Renew. Energ.* 30 (2019) 41–49. <https://doi.org/10.1016/j.renene.2018.06.047>.
- [46] R. Shan, L. Lu, Y. Shi, H. Yuan, J.J. Shi, Catalysts from renewable resources for biodiesel production, *Energ. Convers. Manage.* 178 (2018) 277–289. <https://doi.org/10.1016/j.enconman.2018.10.032>.
- [47] Z.E. Tang, S. Lim, Y.L. Pang, H.C. Ong, K.T. Lee, Synthesis of biomass as heterogeneous catalyst for application in biodiesel production: state of the art and fundamental review, *Renew. Sust. Energ. Rev.* 92 (2018) 235–253. <https://doi.org/10.1016/j.rser.2018.04.056>.
- [48] L.J. Konwar, J. Boro, D. Deka, Review on latest developments in biodiesel production using carbon-based catalysts, *Renew. Sust. Energ. Rev.* 29 (2014) 546–564. <https://doi.org/10.1016/j.biortech.2017.06.163>.
- [49] W.J. Liu, H. Jiang, H.Q. Yu, Development of biochar-based functional materials: toward a sustainable platform carbon material, *Chem. Rev.* 115 (2015) 12251–12285. <https://doi.org/10.1021/acs.chemrev.5b00195>.
- [50] Y. Zu, G. Liu, Z. Wang, J. Shi, M. Zhang, W. Zhang, M. Jia, CaO supported on porous carbon as highly efficient heterogeneous catalysts for transesterification of triacetin with methanol, *Energ. Fuel* 24 (2010) 3810–3816. <https://doi.org/10.1021/ef100419>.
- [51] M. Hara, Environmentally benign production of biodiesel using heterogeneous catalysts, *ChemSusChem* 2 (2009) 129–135. <https://doi.org/10.1002/cssc.200800222>.
- [52] FAOSTAT. Food and Agriculture Organization of the United Nations. <http://www.fao.org/faostat/en/#data/QC>, 2019 (accessed 12 January 2020).

- [53] Secretaría de Economía Monografía del Sector Aguacate en México: Planeación Agrícola Nacional 2017-2030. Aguacate Mexicano.  
<https://www.gob.mx/cms/uploads/attachment/file/257067/Potencial-Aguacate.pdf>, 2019 (accessed 12 January 2020).
- [54] W. Wang, T.R. Bostic, L. Gu, Antioxidant capacities, procyanidins and pigments in avocados of different strains and cultivars, *Food Chem.* 122 (2010) 1193–1198. <https://doi.org/10.1016/j.foodchem.2010.03.114>.
- [55] M.Á. Salomón-Negrete, H.E. Reynel-Ávila, D.I. Mendoza-Castillo, A. Bonilla-Petriciolet, C.J. Duran-Valle, Water defluoridation with avocado-based adsorbents: Synthesis, physicochemical characterization and thermodynamic studies, *J. Mol. Liq.* 254 (2018) 188–197.  
<https://doi.org/10.1016/j.molliq.2018.01.084>.
- [56] E.E. Merodio-Morales, H.E. Reynel-Ávila, D.I. Mendoza-Castillo, C. J. Duran-Valle, A. Bonilla-Petriciolet, Lanthanum- and cerium-based functionalization of chars and activated carbons for the adsorption of fluoride and arsenic ions, *Int. J. Environ. Sci. Technol.* 17 (2020) 115–128.  
<https://doi.org/10.1007/s13762-019-02437-w>.
- [57] L. di Bitonto, C. Pastore, Metal hydrated-salts as efficient and reusable catalysts for pre-treating waste cooking oils and animal fats for an effective production of biodiesel, *Renew. Energ.* 143 (2019) 1193–1200.  
<https://doi.org/10.1016/j.renene.2019.05.100>.
- [58] R. Leyva-Ramos, L.E. Landin-Rodriguez, S. Leyva-Ramos, N.A. Medellin-Castillo NA, Modification of corncob with citric acid to enhance its capacity for adsorbing cadmium (II) from water solution, *Chem. Eng. J.* 180 (2012) 113–120. <https://doi.org/10.1016/j.cej.2011.11.021>.

- [59] P.W.P.A. Valle, T.F. Rezende, R.A. Souza, I.C.P. Fortes, V.M.D. Pasa, Combination of Fractional Factorial and Doehlert Experimental Designs in Biodiesel Production: Ethanolysis of *Raphanus sativus* L. var. *oleiferus* Stokes Oil Catalyzed by Sodium Ethoxide. *En. Fuel.* 23 (2009) 5219–5227. <https://doi.org/10.1021/ef900468p>
- [60] L. di Bitonto, A. Lopez, G. Mascolo, G. Mininni, C. Pastore, Efficient solvent-less separation of lipids from municipal wet sewage scum and their sustainable conversion into biodiesel, *Renew. Energ.* 90 (2016) 55–61. <https://doi.org/10.1016/j.renene.2015.12.049>.
- [61] C. Pastore, A. Lopez, G. Mascolo, Efficient conversion of brown grease produced by municipal wastewater treatment plant into biofuel using aluminium chloride hexahydrate under very mild conditions, *Bioresour. Technol.* 155 (2014) 91–97. <https://doi.org/10.1016/j.biortech.2013.12.106>.
- [62] B. Likozar, J. Levec, Transesterification of canola, palm, peanut, soybean and sunflower oil with methanol, ethanol, isopropanol, butanol and tert-butanol to biodiesel: Modelling of chemical equilibrium, reaction kinetics and mass transfer based on fatty acid composition, *Appl. Energ.*, 123 (2014) 108–120. <https://doi.org/10.1016/j.apenergy.2014.02.046>.
- [63] M. Diasakou, A. Louloudi, N. Papayannakos, Kinetics of the non-catalytic transesterification of soybean oil, *Fuel*, 77, 1297–1302. [https://doi.org/10.1016/S0016-2361\(98\)00025-8](https://doi.org/10.1016/S0016-2361(98)00025-8).
- [64] A. Mondala, K. Liang, H. Toghiani, R. Hernandez, T. French, Biodiesel production by in situ transesterification of municipal primary and secondary sludges, *Bioresour. Technol.* 100 (2009) 1203–1210. <https://doi.org/10.1016/j.biortech.2008.08.020>.

- [65] M. Razavy, Quantum Theory of Tunneling, 1st ed., World Scientific Publishing Company, Singapore, 2003.
- [66] C. Pastore, E. Barca, G. Del Moro, A. Lopez, G. Mininni, G. Mascolo, Recoverable and reusable aluminium solvated species used as a homogeneous catalyst for biodiesel production from brown grease, Appl. Catal. A: Gen. 501 (2015) 48–55. <https://doi.org/10.1016/j.apcata.2015.04.031>.
- [67] H. Trautmann, C. Weihs, On the distribution of the desirability index using Harrington's desirability function, Metrika 63 (2006) 207–213. <https://doi.org/10.1007/s00184-005-0012-0>.
- [68] L. di Bitonto, H.E. Reynel-Avila, D.I. Mendoza-Castillo, A. Bonilla-Petriciolet,, C. Pastore, Residual Mexican biomasses for bioenergy and fine chemical production: correlation between composition and specific applications. Biomass Conv. Bioref. (2020). <https://doi.org/10.1007/s13399-020-00616-1>.
- [69] A. Kosińska, M. Karamać, I. Estrella, T. Hernández, B. Bartolomé, G.A. Dykes, Phenolic compound profiles and antioxidant capacity of Persea americana Mill. peels and seeds of two varieties, J. Agr. Food Chem. 60 (2012) 4613–4619. <https://doi.org/10.1021/jf300090p>.
- [70] I. Demiral, E.A. Ayan, Pyrolysis of grape bagasse: Effect of pyrolysis conditions on the product yields and characterization of the liquid product, Bioresour. Technol. 102 (2011) 3946-3951. <https://doi.org/10.1016/j.biortech.2010.11.077>.
- [71] J.F. González, S. Román, J.M. Encinar, G. Martínez, Pyrolysis of various biomass residues and char utilization for the production of activated carbons, J. Anal. Appl. Pyrol., 85 (2009) 134-141. doi:10.1016/j.jaap.2008.11.035
- [72] X. Shi, J. Wang, A comparative investigation into the formation behaviors of char, liquids and gases during pyrolysis of pinewood and lignocellulosic

- components, Bioresour. Technol. 170 (2014) 262–269. doi:10.1016/j.biortech.2014.07.110
- [73] G. Sahu, N.K. Gupta, A. Kotha, S. Saha, S. Datta, P. Chavan, N. Kumari, P. Dutta, A Review on Biodiesel Production through Heterogeneous Catalysis Route, ChemBioEng Reviews 5 (2018) 231-252. doi:10.1002/cben.201700014
- [74] J.F. Figueiredo, M.F.R. Pereira, M.M.A. Freitas, J.J.M. Orfao, Modification of the surface chemistry of activated carbons, Carbon 27 (1999) 1379–1389. [http://dx.doi.org/10.1016/S0008-6223\(98\)00333-9](http://dx.doi.org/10.1016/S0008-6223(98)00333-9).
- [75] E. Barbosa-Martín, L. Chel-Guerrero, E. González-Mondragón, D. Betancur-Ancona, Chemical and technological properties of avocado (Persea americana Mill.) seed fibrous residues, Food Bioprod. Process. 100 (2016) 457–463. <https://doi.org/10.1016/j.fbp.2016.09.006>.
- [76] M.P. Elizalde-González, J. Mattusch, A.A. Peláez-Cid, R. Wennrich, Characterization of adsorbent materials prepared from avocado kernel seeds: Natural, activated and carbonized forms, J. Anal. Appl. Pyrol. 78 (2007) 185–193. <https://doi.org/10.1016/j.jaap.2006.06.008>.
- [77] Y.M. Evtushenko, V.M. Ivanov, B.E. Zaitsev, Determination of epoxide and hydroxyl groups in epoxide resins by IR spectrometry, J. Anal. Chem. 58 (2003) 347–350. <https://doi.org/10.1023/A:1023297731492>.
- [78] M. Kouzu, T. Kasuno, M. Tajika, S. Yamanaka, J. Hidaka, Active phase of calcium oxide used as solid base catalyst for transesterification of soybean oil with refluxing methanol, Appl. Catal. A: Gen. 334 (2008) 357–365. <https://doi.org/10.1016/j.apcata.2007.10.023>.
- [79] P.E. Halstead, A.E Moore, The thermal dissociation of calcium hydroxide, J. Chem. Soc. 769 (1957) 3873–3875. <https://doi.org/10.1039/JR9570003873>.

- [80] M. Morgenstern, J. Cline, S. Meyer, S. Cataldo, Determination of the kinetics of biodiesel production using proton nuclear magnetic resonance spectroscopy ( $^1\text{H}$  NMR), *Energ. Fuel* 20 (2006) 1350–1353.  
<https://doi.org/10.1021/ef0503764>.
- [81] T. Thakkar, K. Shah, P. Kodgire, S.S. Kachhwaha, In-situ reactive extraction of castor seeds for biodiesel production using the coordinated ultrasound–microwave irradiation: Process optimization and kinetic modeling, *Ultrason. Sonochem.* 50 (2019) 6–14. <https://doi.org/10.1016/j.ultsonch.2018.08.007>.
- [82] M. Casiello, L. Catucci, F. Fracassi, C. Fusco, A.G. Laurenza, L. di Bitonto, C. Pastore, L. D'Accolti, A. Nacci, *Catalysts* 9 (2019) 71–84.  
<https://doi.org/10.3390/catal9010071>.
- [83] L. Li, N. Yi, X. Wang, X. Lin, T. Zeng, T. Qiu, Novel triazolium-based ionic liquids as effective catalysts for transesterification of palm oil to biodiesel, *J. Mol. Liq.* 249 (2018) 732–738. <https://doi.org/10.1016/j.molliq.2017.11.097>.
- [84] Y. Feng, T. Qiu, J. Yang, L. Li, X. Wang, H. Wang, Transesterification of palm oil to biodiesel using Brønsted acidic ionic liquid as high-efficient and eco-friendly catalyst, *Chin. J. Chem. Eng.* 25 (2017) 1222–1229.  
<https://doi.org/10.1016/j.cjche.2017.06.027>.
- [85] V. Volli, M.K. Purkait, Preparation and characterization of hydrotalcite-like materials from flyash for transesterification, *Clean. Technol. Environ. Policy*, 18 (2016) 529–540. <https://doi.org/10.1007/s10098-015-1036-4>.
- [86] G. Paterson, T. Issariyakul, C. Baroi, A. Bassi, A. Dalai, Ion-exchange resins as catalysts in transesterification of triolein, *Catal. Today* 212 (2013) 157–163.  
<https://doi.org/10.1016/j.cattod.2012.10.013>.
- [87] M. Feyzi, G. Khajavi, Kinetics study of biodiesel synthesis from sunflower oil using Ba-Sr/ZSM-5 nanocatalyst, *Iran J. Catal.* 6 (2016) 29–35.

- [88] G. Moradi, M. Mohadesi, Z. Hojabri, Biodiesel production by CaO/SiO<sub>2</sub> catalyst synthesized by the sol–gel process, *React. Kinet. Catal. Lett.* 113 (2014) 169–186. <https://doi.org/10.1007/s11144-014-0728-9>.
- [89] D. Kumar, A. Ali, Transesterification of low-quality triglycerides over a Zn/CaO heterogeneous catalyst: kinetics and reusability studies, *Energ. Fuel* 27 (2013) 3758–3768. <https://doi.org/10.1021/ef400594t>.

### Figure caption

**Fig 1.** a) FTIR and b) XRD spectra of biochar and carbon-based calcium catalysts.

**Fig 2.** SEM images of biochar and nanostructures of calcium oxides deposited on avocado char.

**Fig 3.** a) Catalytic activity of carbon-based calcium catalysts in the transesterification reaction of sunflower oil with methanol, b) correlation between FAME content (wt.%) and their basic/acid properties. Reaction conditions: molar ratio methanol to oil = 15, weight ratio catalyst to oil= 5%, 100 °C, 3 h.

**Fig 4.** a) Kinetic studies of the transesterification reaction of sunflower oil with methanol by using supported catalyst with 20 wt.% of Ca loaded. Linear interpolations of b) pseudo-first order and c) pseudo-second order. Reaction conditions: molar ratio methanol to oil = 15, weight ratio catalyst to oil = 5%, temperature from 60 to 100 °C, time = 5 h.

**Fig 5.** Linear plot of Arrhenius equation for the determination of activation energy ( $E_a$ ).

**Fig 6.** Linear plot of Eyring–Polanyi equation for the determination of thermodynamic parameters ( $\Delta^\ddagger H$ ,  $\Delta^\ddagger S$  and  $\Delta^\ddagger G$ ).

**Fig 7.** Response surface plot of the combined effects of: (a) temperature and reaction time (molar ratio methanol to oil = 10, weight ratio catalyst to oil = 5%), (b) catalyst concentration and temperature (molar ratio methanol to oil = 10, time = 3 h), (c) molar ratio methanol to oil and reaction time (weight ratio catalyst to oil = 5%, temperature = 80 °C), (d) catalyst concentration and molar ratio methanol to oil (time = 3 h, temperature = 80 °C).

**Fig 8.** Recycling tests of supported catalyst with 20 wt.% of Ca loaded. a) Direct reuse and b) after thermal activation at 550 °C under N<sub>2</sub> flow. Reaction conditions: molar ratio MeOH to pre-treated oil = 15.6, weight ratio catalyst to oil = 7.3 wt.%, 99.5 °C, 5 h.

**Fig 9.** a) XRD and b) FTIR of supported catalyst with 20 wt.% of Ca loaded before and at the end of the third cycle of reaction. Reaction conditions: molar ratio methanol to pre-treated oil = 15.6, weight ratio catalyst to pre-treated oil = 7.3 wt.%, 99.5 °C, 5 h.

**Fig 10.** Kinetic of transesterification of pre-treated WCO by using supported catalyst with 20% of Ca loaded. Reaction conditions: molar ratio MeOH to esterified WCO = 15.6, catalyst = 7.3 wt.%, 99.5 °C, 5 h.



**Fig. 1**

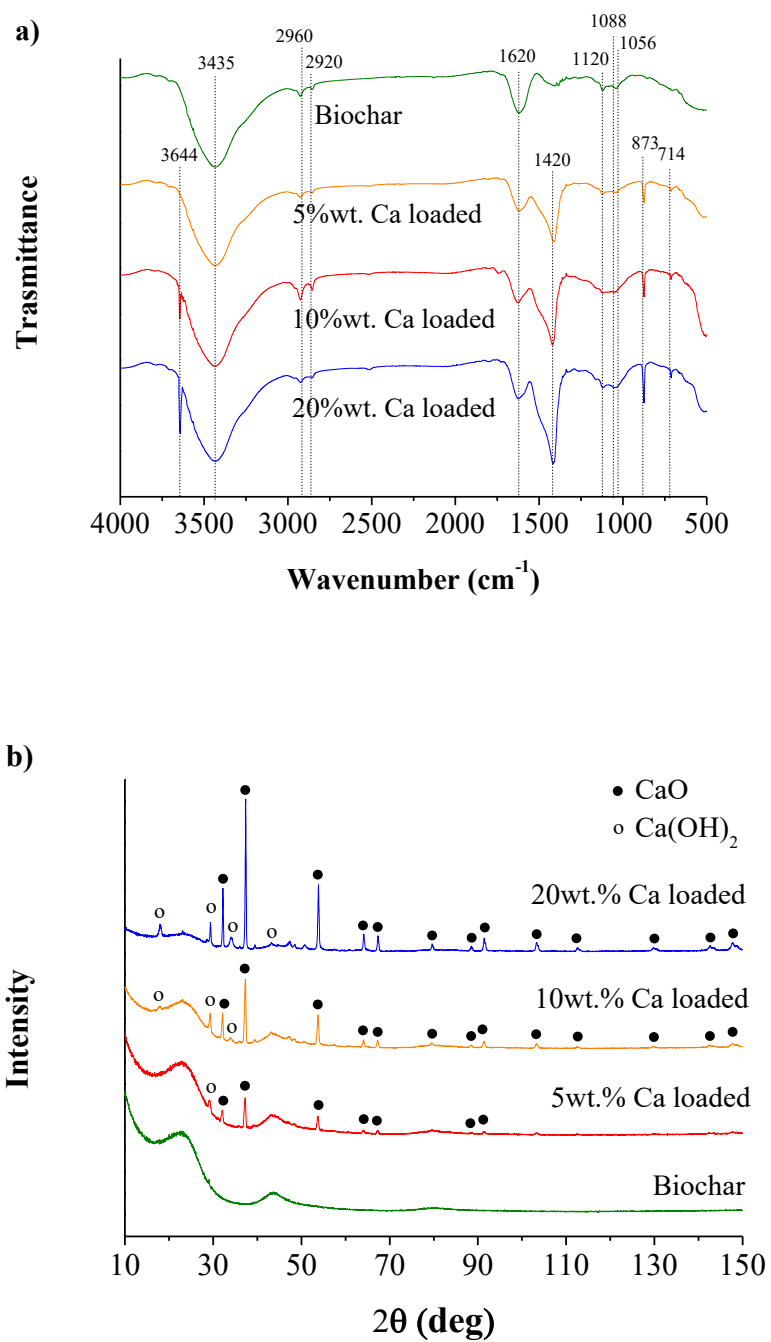
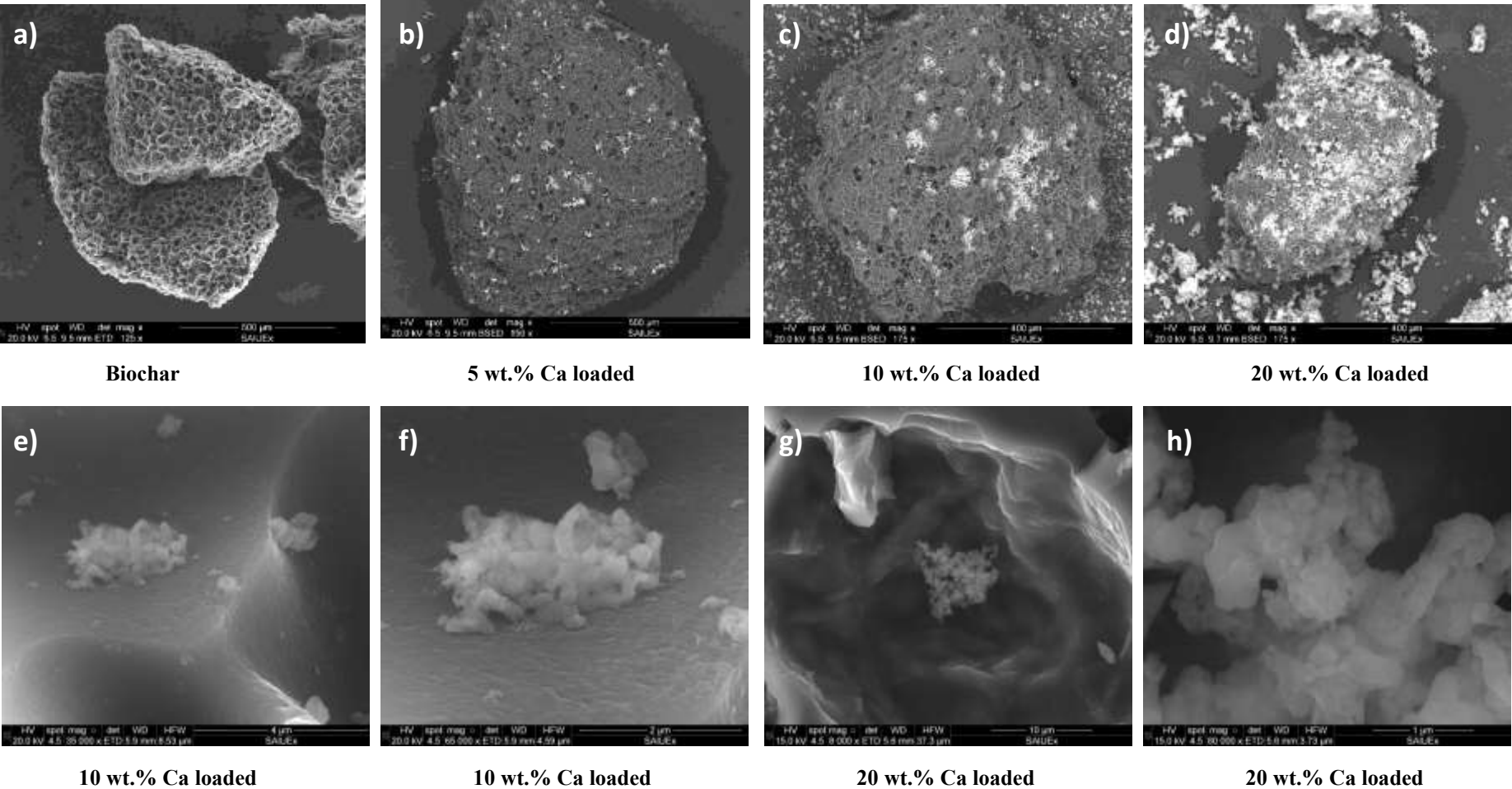
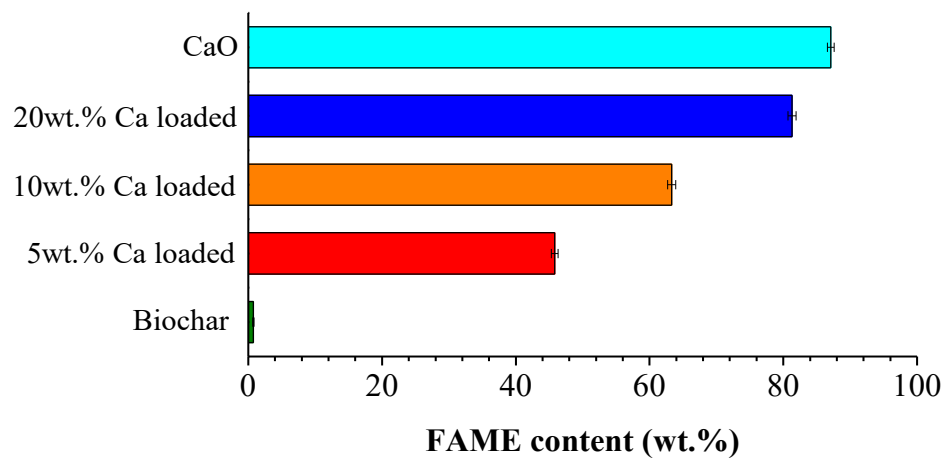


Fig. 2

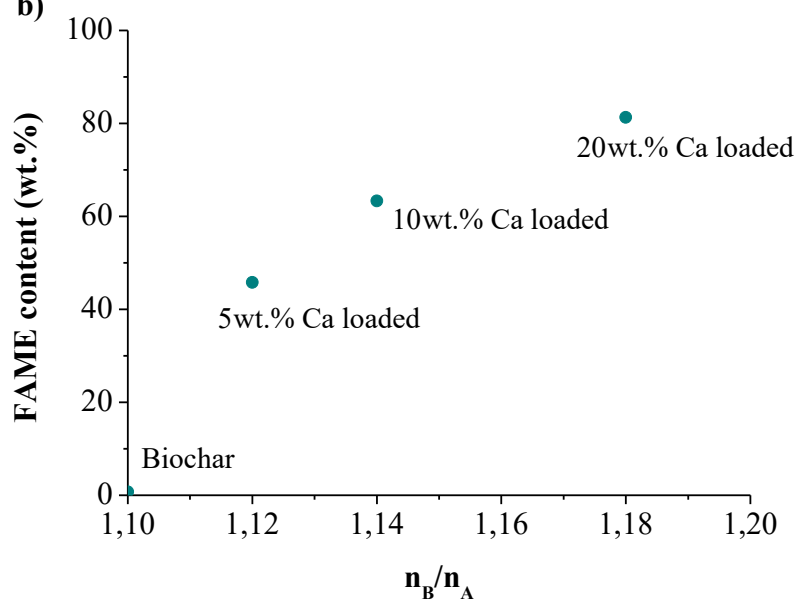


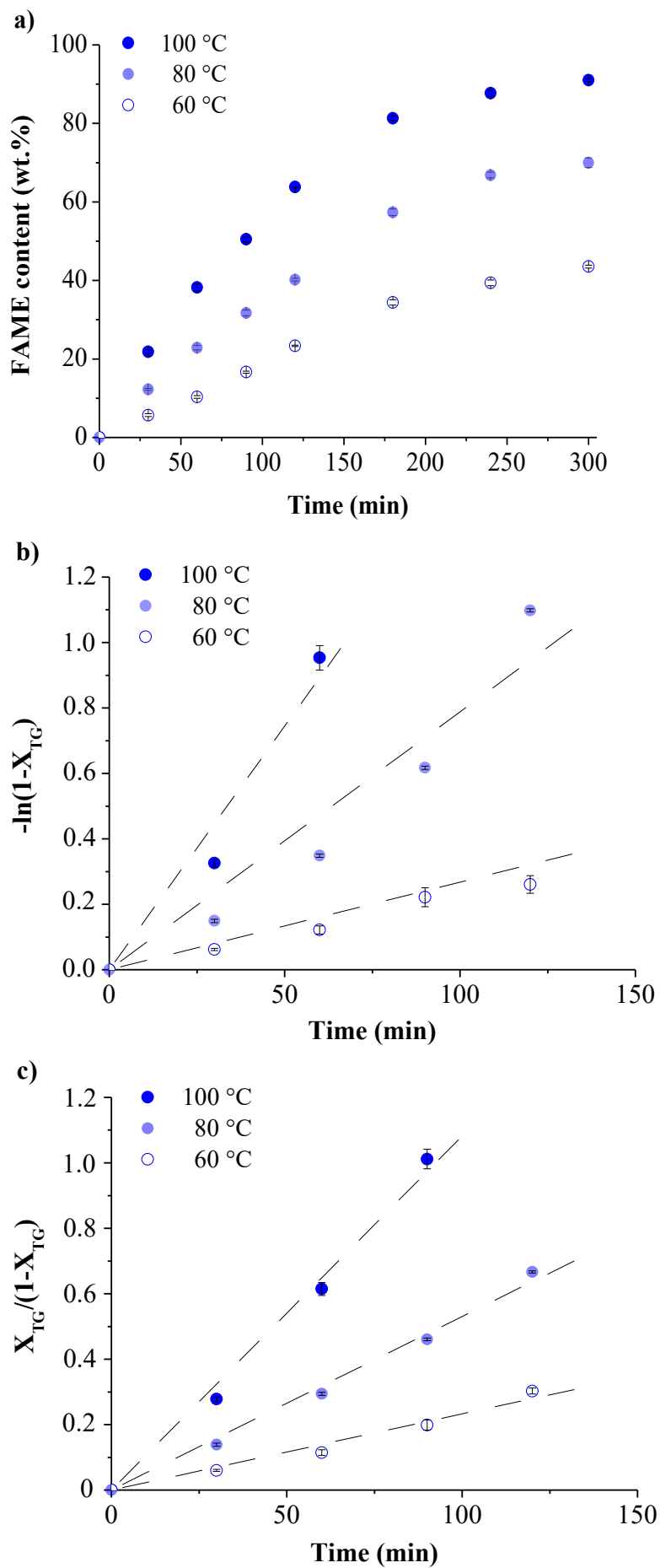
**Fig. 3**

**a)**



**b)**



**Fig. 4**


**Fig. 5**

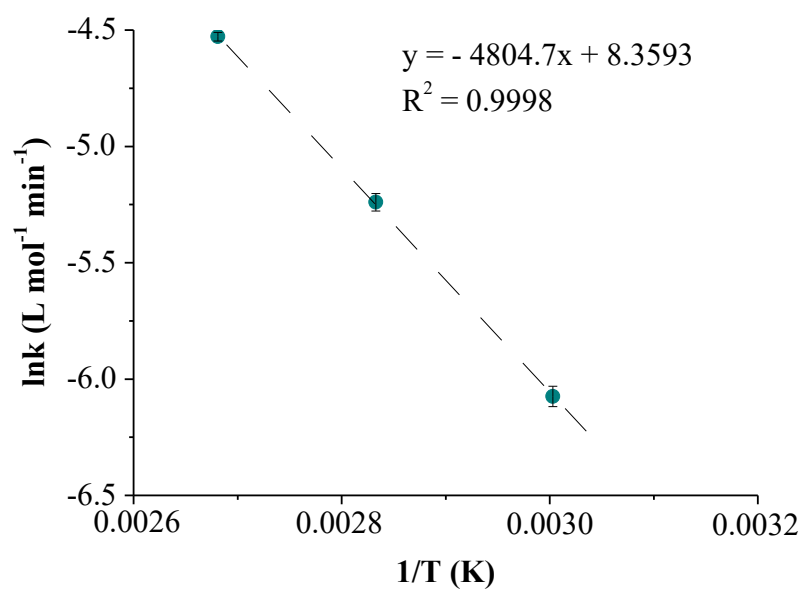


**Fig. 6**

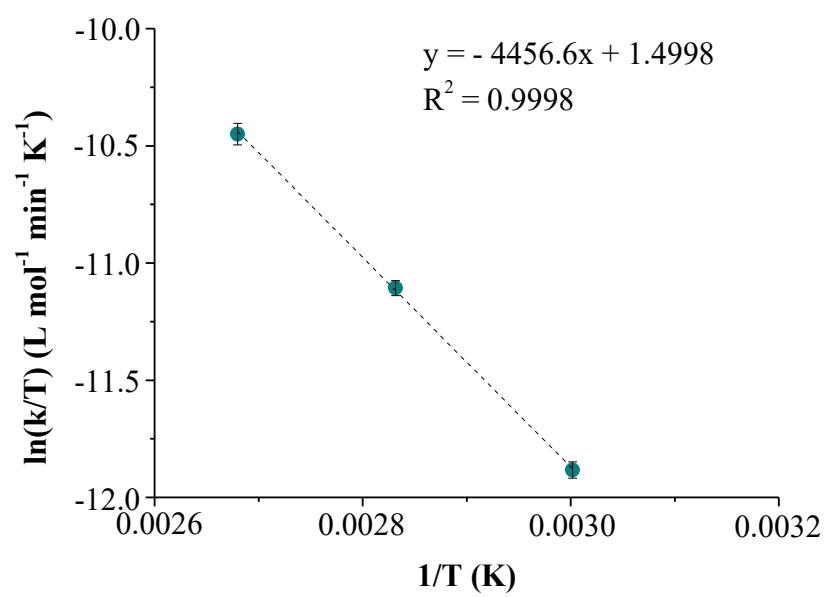
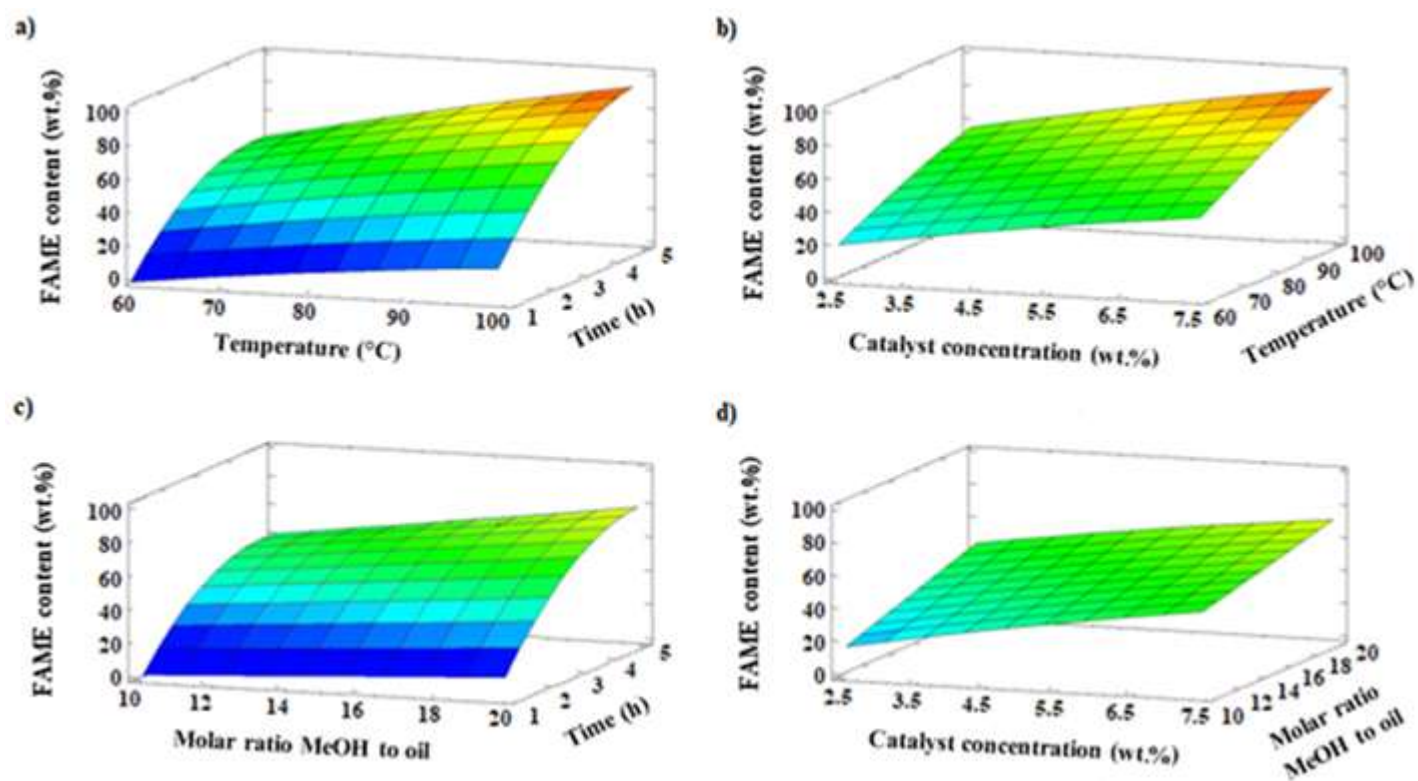
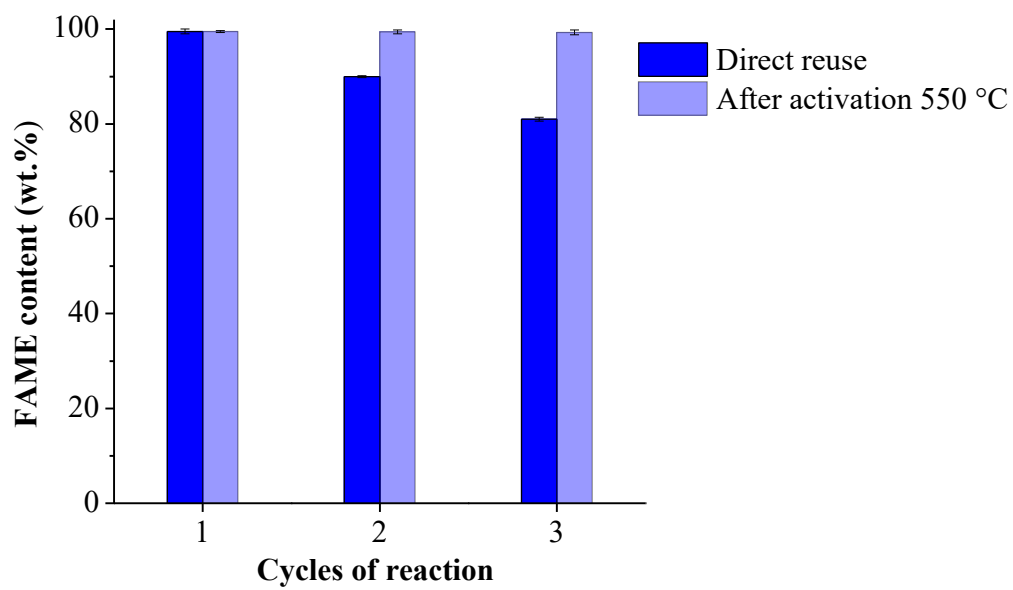


Fig. 7



**Fig. 8**





**Fig. 9**

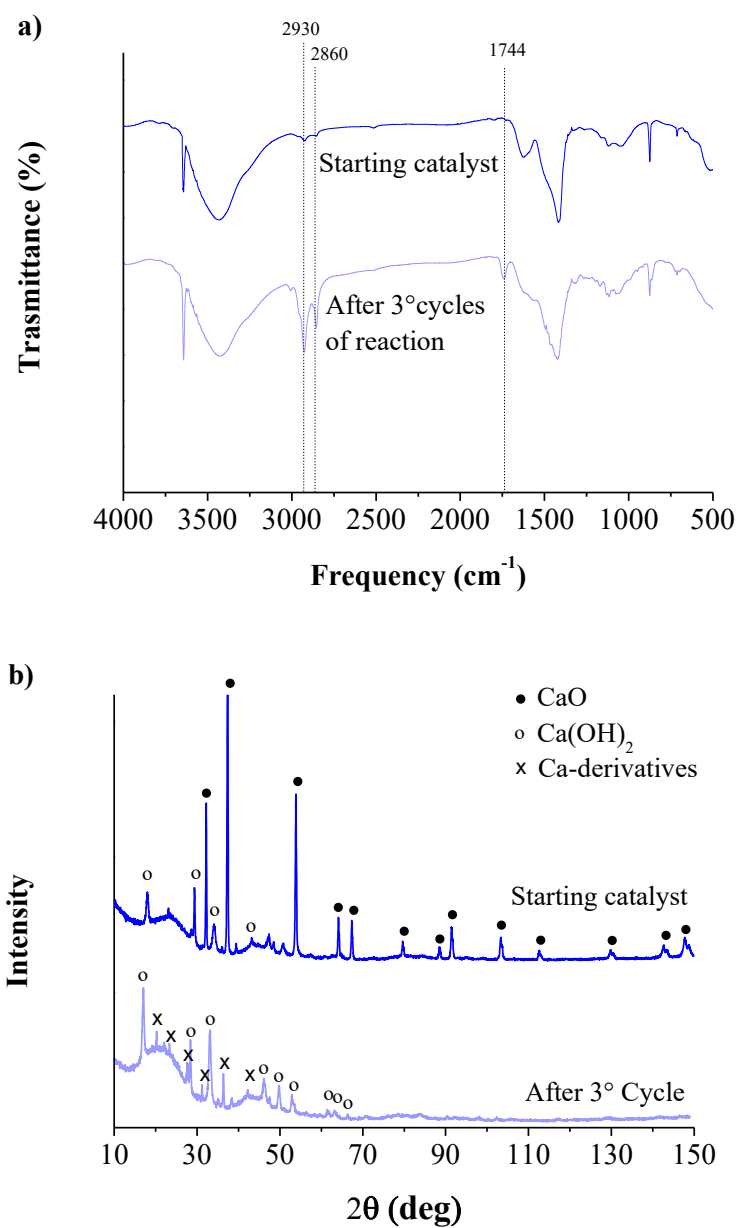


**Fig. 10**

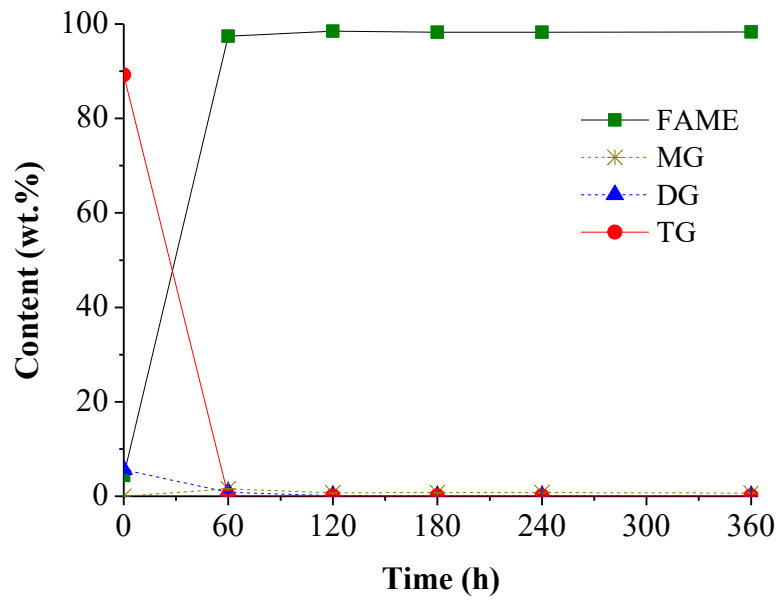


**Table 1.**

Elemental analysis (wt.%) of biochar and carbon-based calcium catalysts.

<b>E</b>	<b>Samples</b>	<b>Element (wt.%)</b>						
		<b>C</b>	<b>H</b>	<b>N</b>	<b>S</b>	<b>O</b>	<b>Ca</b>	<b>Others</b>
1	Biochar	85.03	2.15	1.99	0.05	10.78	-	-
2	5 wt.% Ca loaded	84.10	2.02	1.61	0.04	9.53	2.26	0.44
3	10 wt.% Ca loaded	79.47	1.59	1.49	0.03	10.56	6.39	0.47
4	20 wt.% Ca loaded	63.85	2.17	1.26	0.03	20.30	12.0	0.39

**Table 2.**

Average pore diameter (nm), pore volume, pore volume ( $\text{cm}^3 \text{ g}^{-1}$ ) and surface area ( $\text{m}^2 \text{ g}^{-1}$ ) for biochar and carbon-based calcium catalysts.

<b>E</b>	<b>Samples</b>	<b>Average pore diameter (nm)</b>	<b>Pore volume (<math>\text{cm}^3 \text{ g}^{-1}</math>)</b>	<b>Surface area (<math>\text{m}^2 \text{ g}^{-1}</math>)</b>
1	Biochar	4.29	0.03	12
2	5 wt.% Ca loaded	1.14	0.04	28
3	10 wt.% Ca loaded	1.30	0.04	16
4	20 wt.% Ca loaded	0.53	0.19	253

**Table 3.**

Rate constants ( $k$ ) and coefficients of determination ( $R^2$ ) for the pseudo-first and pseudo-second order reactions.

Temperature (K)	Pseudo-first order		Pseudo-second order	
	$k_1 (10^{-2})$ (min <sup>-1</sup> )	$R_1^2$	$k_2 (10^{-2})$ (L mol <sup>-1</sup> min <sup>-1</sup> )	$R_2^2$
373.15	1.49 ± 0.05	0.9612	1.08 ± 0.02	0.9916
353.15	0.79 ± 0.02	0.9270	0.53 ± 0.02	0.9952
333.15	0.27 ± 0.03	0.9530	0.23 ± 0.01	0.9847

**Table 4.**

Previous studies of kinetics for the transesterification process.

<b>E</b>	<b>Feedstocks</b>	<b>Acidity (wt.%)</b>	<b>Catalyst</b>	<b><i>E<sub>a</sub></i> (kJ mol<sup>-1</sup>)</b>	<b>Reference</b>
1	Sunflower oil	-	NaOH	27.2	[80]
2	Castor oil	1.2	KOH	28.3	[81]
3	Soybean oil	1	ZnO/TBAI	48.5	[82]
4	Palm oil	0.3	[Taz-prSO <sub>3</sub> H][CF <sub>3</sub> SO <sub>3</sub> ]	86.5	[83]
5	Palm oil	0.2	[CyN <sub>1,1</sub> PrSO <sub>3</sub> H][p-TSA]	122.9	[84]
6	Mustard oil	-	Hydrotalcites Mg-Al	130.5	[85]
7	Triolein	0.1	Amberlyst 15	120	[86]
8	Sunflower oil	-	Ba-Sr/ZSM-5	67.0	[87]
9	Corn oil	0.5	CaO/SiO <sub>2</sub>	49.9	[88]
10	Cotton seed oil	1.3	Zn/CaO	43.0	[89]
11	Sunflower oil	0.3	20 wt.% Ca loaded	39.9	In this study

**Table 5.**

Thermodynamic parameters of activation for the transesterification reaction catalyzed by supported catalyst with 20 wt.% of Ca loaded.

Temperature (K)	Thermodynamic parameters		
	$\Delta^\ddagger H$ (kJ·mol <sup>-1</sup> )	$\Delta^\ddagger S$ (kJ·mol <sup>-1</sup> ·K)	$\Delta^\ddagger G$ (kJ·mol <sup>-1</sup> )
373.15	37.05	-0.185	106.08
353.15			102.38
333.15			98.68

**Table 6.**

Box–Behnken design matrix for the four independent variables and the experimental FAME content.

<b>E</b>	<b>Molar ratio methanol to oil</b>	<b>Catalyst concentration (wt.%)</b>	<b>Temperature (°C)</b>	<b>Time (h)</b>	<b>FAME content (wt.%)</b>
1	10	5.0	60	3	18.2
2	15	7.5	100	3	91.2
3	20	2.5	80	3	47.2
4	10	5.0	100	3	70.2
5	20	5.0	80	1	29.1
6	15	5.0	100	5	91.0
7	20	5.0	100	3	87.0
8	10	5.0	80	1	10.2
9	15	2.5	100	3	53.2
10	20	7.5	80	3	78.4
11	15	5.0	80	3	57.4
12	10	5.0	80	5	52.1
13	15	7.5	60	3	50.0
14	10	7.5	80	3	68.4
15	15	7.5	80	1	28.2
16	10	2.5	80	3	30.2
17	15	2.5	60	3	18.2
18	15	5.0	80	3	56.5
19	15	5.0	60	5	43.4
20	15	5.0	60	1	6.3
21	15	5.0	80	3	58.2
22	15	2.5	80	1	12.3
23	15	2.5	80	5	50.2
24	20	5.0	80	5	87.2
25	15	5.0	100	1	32.9
26	20	5.0	60	3	50.1
27	15	7.5	80	5	89.2



**Table 7.**

The ANOVA summary.

Source	Sum of Squares	Df	Mean Square	F-Ratio	P-Value
<i>Model</i>	16526.2	14	4131.55	67.61	0.0000*
<i>Cat</i>	1581.67	1	1581.67	102.36	0.0000**
<i>C</i>	1104.68	1	1104.68	71.49	0.0000**
<i>T</i>	1802.41	1	1802.41	116.65	0.0000**
<i>T</i>	3281.63	1	3281.63	212.38	0.0000**
<i>catC</i>	12.0756	1	12.0756	0.78	0.3940
<i>catT</i>	13.1044	1	13.1044	0.85	0.3752
<i>Catt</i>	133.634	1	133.634	8.65	0.0124**
<i>CT</i>	57.3049	1	57.3049	3.71	0.0782
<i>Ct</i>	65.529	1	65.529	4.24	0.0618
<i>Tt</i>	110.986	1	110.986	7.18	0.0200**
<i>cat<sup>2</sup></i>	11.1105	1	11.1105	0.72	0.4130
<i>C<sup>2</sup></i>	0.101445	1	0.101445	0.01	0.9368
<i>T<sup>2</sup></i>	22.9265	1	22.9265	1.48	0.2466
<i>t<sup>2</sup></i>	752.981	1	752.981	48.73	0.0000**
Total error	185.419	12	15.4516		
Total (corr.)	17974.4	26			

 $R^2 = 98.97\%$  \* $P < 0.05$  indicates model is significant $R^2(\text{adjusted for d.f.}) = 97.76$  \*\* $P < 0.05$  indicates model terms are significant

**Table 8.**

Composition of waste cooking oil (WCO) and esterified WCO by using  $\text{AlCl}_3 \cdot 6\text{H}_2\text{O}$  as catalyst.

Sample	FFAs (mg KOH g <sup>-1</sup> )	FAME (wt.%)	MG (wt.%)	DG (wt.%)	TG (wt.%)
WCO	8.05 ± 0.04	-	0.8 ± 0.1	3.9 ± 0.1	90.9 ± 0.3
Pretreated WCO	0.77 ± 0.02	4.4 ± 0.3	-	5.6 ± 0.1	89.2 ± 0.2

**Table 9.**

Comparison of the chemical properties of biodiesel produced during the transesterification process by using supported catalyst with 20 wt.% of Ca loaded and EN14214 standard.

Properties	Biodiesel	EN14214	
		Lower limit	Upper limit
Ester content (wt.%)	98.3	96.5	-
Water content (mg kg <sup>-1</sup> )	100	-	500
Acid value (mg KOH g <sup>-1</sup> )	0.1	-	0.5
Methanol content (wt.%)	-	-	0.2
Monoglycerides content (wt.%)	0.6	-	0.7
Diglycerides content (wt.%)	0.1	-	0.2
Triglycerides content (wt.%)	0.1	-	0.2
Free Glycerine (wt.%)	-	-	0.02
Total Glycerine (wt.%)	-	-	0.25
Group I metals (Na+K)	-	-	5
Group II metal (Ca+Mg)	-	-	5